

Annual Review of Marine Science

Earth, Wind, Fire, and Pollution: Aerosol Nutrient Sources and Impacts on Ocean Biogeochemistry

Douglas S. Hamilton,¹ Morgane M.G. Perron,²
Tami C. Bond,³ Andrew R. Bowie,²
Rebecca R. Buchholz,⁴ Cecile Guieu,⁵ Akinori Ito,⁶
Willy Maenhaut,⁷ Stelios Myriokefalitakis,⁸
Nazlı Olgun,⁹ Sagar D. Rathod,¹⁰ Kerstin Schepanski,¹¹
Alessandro Tagliabue,¹² Robert Wagner,¹³
and Natalie M. Mahowald¹

¹Department of Earth and Atmospheric Science, Cornell University, Ithaca, New York 14853, USA; email: dsh224@cornell.edu

²Institute for Marine and Antarctic Studies, University of Tasmania, Battery Point, Tasmania 7004, Australia

³Department of Mechanical Engineering, Colorado State University, Fort Collins, Colorado 80521, USA

⁴Atmospheric Chemistry Observations and Modeling Laboratory, National Center for Atmospheric Research, Boulder, Colorado 80301, USA

⁵Laboratoire d'Océanographie de Villefranche, Sorbonne Université, CNRS, 06230 Villefranche-sur-Mer, France

⁶Yokohama Institute for Earth Sciences, Japan Agency for Marine-Earth Science and Technology, Yokohama, Kanagawa 236-0001, Japan

⁷Department of Chemistry, Ghent University, 9000 Ghent, Belgium

⁸Institute for Environmental Research and Sustainable Development, National Observatory of Athens, 15236 Penteli, Greece

⁹Climate and Marine Sciences Division, Eurasia Institute of Earth Sciences, Istanbul Technical University, 34469 Maslak, Istanbul, Turkey

¹⁰Department of Atmospheric Science, Colorado State University, Fort Collins, Colorado 80521, USA

¹¹Institute of Meteorology, Freie Universität Berlin, 12165 Berlin, Germany

¹²School of Environmental Sciences, University of Liverpool, Liverpool L69 3GP, United Kingdom

¹³Leibniz Institute for Tropospheric Research, 04318 Leipzig, Germany

 **ANNUAL
REVIEWS CONNECT**

www.annualreviews.org

- Download figures
- Navigate cited references
- Keyword search
- Explore related articles
- Share via email or social media

Annu. Rev. Mar. Sci. 2022. 14:303–30

First published as a Review in Advance on
August 20, 2021

The *Annual Review of Marine Science* is online at
marine.annualreviews.org

<https://doi.org/10.1146/annurev-marine-031921-013612>

Copyright © 2022 by Annual Reviews.
All rights reserved

Keywords

mineral dust, fires, volcanoes, phosphate, soluble iron, ocean biogeochemistry

Abstract

A key Earth system science question is the role of atmospheric deposition in supplying vital nutrients to the phytoplankton that form the base of marine food webs. Industrial and vehicular pollution, wildfires, volcanoes, biogenic debris, and desert dust all carry nutrients within their plumes throughout the globe. In remote ocean ecosystems, aerosol deposition represents an essential new source of nutrients for primary production. The large spatiotemporal variability in aerosols from myriad sources combined with the differential responses of marine biota to changing fluxes makes it crucially important to understand where, when, and how much nutrients from the atmosphere enter marine ecosystems. This review brings together existing literature, experimental evidence of impacts, and new atmospheric nutrient observations that can be compared with atmospheric and ocean biogeochemistry modeling. We evaluate the contribution and spatiotemporal variability of nutrient-bearing aerosols from desert dust, wildfire, volcanic, and anthropogenic sources, including the organic component, deposition fluxes, and oceanic impacts.

INTRODUCTION

By traveling long distances with the atmospheric flow, aerosols deliver essential nutrients to remote marine ecosystems (Baker & Jickells 2017, Doney et al. 2009, Duce et al. 1991, Jickells et al. 2005, Kanakidou et al. 2012, Mahowald et al. 2018). Aerosol transport pathways and distance traveled are determined by a particle's properties (size, composition, and density), atmospheric conditions (particle uplift and buoyancy and wind speed and direction), and travel altitude. The smaller the particle is and the higher its altitude of travel is, the greater chance there is for long atmospheric residence times and for reaching remote marine ecosystems (Baker & Croot 2010). The loss of aerosol (gases) from the atmosphere proceeds by two routes: dry (direct) deposition of the aerosol (gaseous species) and wet deposition within precipitation (Baker et al. 2007). At ~ 362 million km^2 , the world's oceans cover $\sim 71\%$ of the Earth's surface, providing a major sink pathway for nutrients and pollutants emitted from land. The atmospheric lifetimes of aerosols range from a few days to weeks (Textor et al. 2006), much shorter than the mixing time within and between hemispheres. Such short atmospheric lifetimes combined with the heterogeneous physicochemical nature of aerosol composition create large spatial and temporal variations among ocean regions in observed aerosol nutrient concentration patterns (**Figure 1**). As understanding of biogeochemical cycles grows, a strong requirement arises for improved knowledge regarding how nutrients from different sources are supplied to marine ecosystems.

Conceptually, aerosol nutrient sources can be split into three groups: The first is natural in origin and includes mineral dust, wildfires, volcanoes, and biological particles (Barkley et al. 2019, Guieu et al. 2005, Jickells et al. 2005, Mahowald et al. 2008, Olgun et al. 2011); the second is anthropogenic emissions (Ito 2015, Ito et al. 2019, Jickells et al. 2017, Krishnamurthy et al. 2009, Luo et al. 2008, Rathod et al. 2020); and the third is the atmospheric transformation of insoluble minerals, of either natural or anthropogenic origin, into soluble (bioavailable) nutrients during transport by acids, organic ligands, and photoreductive processes (Ito 2015, Johnson & Meskhidze 2013, Longo et al. 2016, Shi et al. 2015, Stockdale et al. 2016). In addition to directly providing a new nutrient source, anthropogenic activity modifies the generation of predominately natural aerosols (Ginoux et al. 2012, Hamilton et al. 2018, Mahowald et al. 2010, Ward et al. 2014) and

Aerosol: solid or liquid particles suspended in the atmosphere

Biogeochemical cycles: the ways in which nutrients move through both the biotic and abiotic parts of the Earth system

Anthropogenic emissions: emissions produced by vehicular transportation, fossil fuel or biofuel combustion, mining, agricultural practices, deforestation, or metal smelting

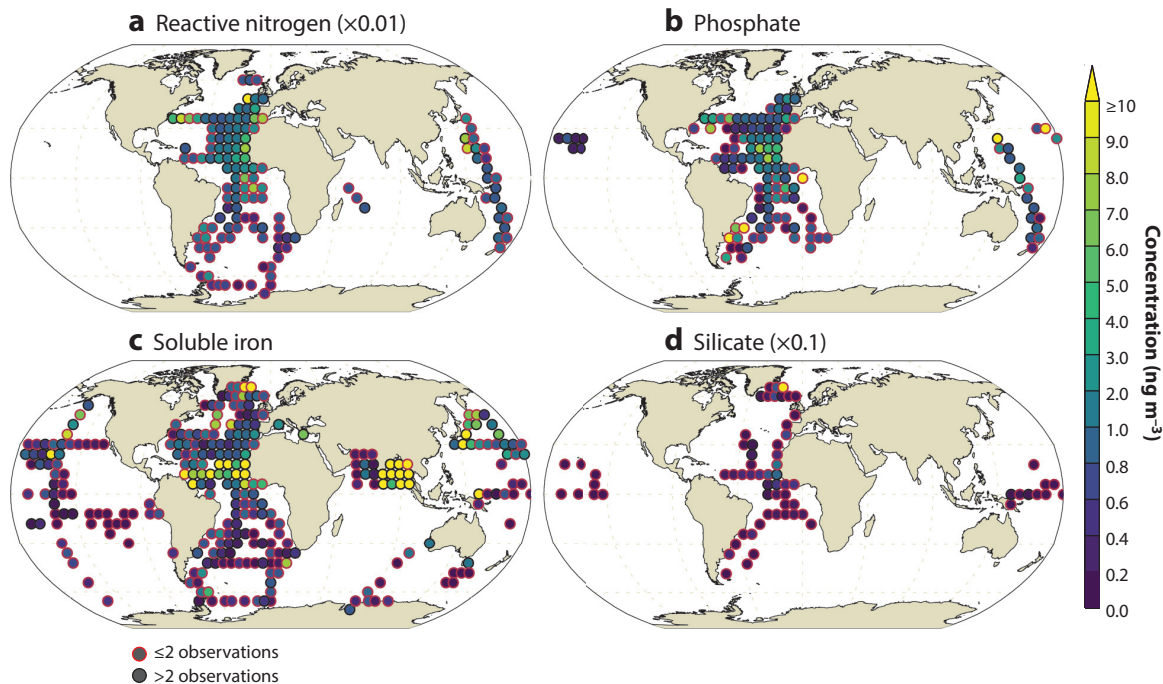


Figure 1

Shipboard observations of the median atmospheric concentrations of (a) reactive nitrogen ($\text{NH}_4 + \text{NO}_3 +$ water-soluble organic nitrogen), (b) phosphate, (c) soluble iron, and (d) silicate. Observations are aggregated over $6^\circ \times 6^\circ$ grid cells. Red outlines indicate two or fewer observations; black outlines indicate more than two observations. Observations of reactive nitrogen, phosphate, and silicate are from Baker et al. (2014); observations of soluble iron are from Hamilton et al. (2019).

provides a source of compounds that work to liberate a fraction of minerals into more bioavailable nutrient forms (Li et al. 2017, Meskhidze et al. 2005, Solmon et al. 2009). This coupling of historical human activity with biogeochemical cycles is highly complex and contains many uncertainties, partly due to the absence of early historical measurements and the reliance on proxy records to describe the historical evolution of natural aerosol fluxes with intensifying human activity.

Marine biota are a key component in the biogeochemical cycles that determine the ocean's capacity to sequester atmospheric CO_2 and support marine ecosystem services over different timescales. Furthermore, they emit biological gases to the atmosphere that subsequently oxidize to form organic and sulfate aerosols, thereby creating climate feedbacks by altering cloud properties, temperatures, and precipitation rates. By relieving nutrient limitation, large aerosol deposition events have the potential to modify the natural assemblage due to new resource competition among primary producers. The resulting change in phytoplankton balance between smaller and larger sizes (Giovagnetti et al. 2013, Paytan et al. 2009) and between autotrophic and heterotrophic communities (Gazeau et al. 2020, Marañón et al. 2010) determines the capacity of the ocean to sequester anthropogenic CO_2 following deposition (Guieu et al. 2014b). The degree to which autotrophs or heterotrophs are stimulated depends on the physicochemical form in which nutrients are delivered to seawater and the initial biogeochemical conditions of the water column, including the initial in situ nutrient limitation linked to the depth and strength of stratification, which determine the supply of macro- or micronutrients from below the thermocline (Guieu et al. 2014a, Marañón et al. 2010). Understanding the fertilization potential of aerosols is of particular

Macronutrients: nitrogen, phosphorus, and silicate

Micronutrients: iron, zinc, copper, cobalt, and manganese

Net primary productivity (NPP):

the biomass accumulation rate from the transformation of energy, in excess of respiration, by photo- or chemosynthesis

Reactive nitrogen:

oxidized, reduced, and organic forms of nitrogen that are bioaccessible; examples include nitrate (NO_3^-) and ammonium (NH_4^+)

Nutrient solubility:

the percentage of the total aerosol that is soluble

interest in surface waters of the Southern Ocean, where phytoplankton net primary productivity (NPP) is limited by iron supply, and the biological response to aerosol deposition can regulate the global carbon cycle (Martin 1990, Parekh et al. 2004, Tagliabue et al. 2014) and the redistribution of macronutrients to low latitudes (Sarmiento et al. 2004, Tagliabue et al. 2009).

There have been several recent efforts to review the most up-to-date knowledge on the magnitude of the atmospheric deposition fluxes of the main nutrient species to the oceans: Altieri et al. (2021) reviewed reactive nitrogen, Jickells et al. (2017) updated anthropogenic nitrogen estimates, Mahowald et al. (2018) reviewed the role of metals as nutrients and pollutants, Myriokefalitakis et al. (2018) undertook a multimodel comparison for soluble iron, and Kanakidou et al. (2018) reviewed nitrogen, phosphorus, and iron chemistry and fluxes. From an oceanic perspective, Boyd & Ellwood (2010) and Tagliabue et al. (2017) reviewed the marine iron cycle, focusing on the impact of mineral dust deposition. Here, we build on this body of literature by reviewing the current understanding of and uncertainties in major aerosol nutrient sources (mainly desert dust, fires, volcanoes, biogenic particles, and anthropogenic activity) and their respective spatiotemporal deposition signatures. While early studies of the impact of atmospheric iron and phosphorus deposition on ocean biogeochemistry often focused solely on dust, recent evidence has highlighted the importance of nondust sources (Barkley et al. 2019, Ito et al. 2019)—even suggesting that the global mean carbon export efficiency (gram of atmospheric CO_2 sequestered per gram of soluble iron deposited) of pyrogenic-sourced iron is six to nine times larger than that of dust-sourced iron (Hamilton et al. 2020a, Ito et al. 2020b). To further explore the emerging role of (wild)fires in biogeochemical cycles, we provide a case study of recent megafire activity in Australia during 2019 and 2020, including recent observations and new atmospheric and ocean biogeochemical modeling experiments. The characterization and individual contributions of differing aeolian pathways to the ocean are important future research areas that require better constraints to improve understanding of the impact of aerosol deposition on marine biogeochemical cycles in the past, present, and future and to better apprehend the fast-evolving human dimension.

AEROSOL NUTRIENTS, OBSERVATIONS OVER OCEANS, AND IMPACTS ON BIOTA

Over the last few decades, intense research efforts such as the Surface Ocean–Lower Atmosphere Study (SOLAS) (<https://www.solas-int.org>) and the GEOTRACES research program (<https://www.geotraces.org>) have significantly advanced understanding of the oceanic impact of nutrient-bearing aerosol deposition. That said, field observations are much more extensive in the Northern Hemisphere due to the easier logistics and cheaper cost of undertaking seagoing campaigns there compared with the Southern Hemisphere (**Figure 1**). As such, the atmospheric deposition fluxes of nutrients to Southern Hemisphere oceans remain highly uncertain, with soluble iron the most studied historically. The highly episodic nature of aeolian dust and wildfire plumes (e.g., the range in daily iron deposition may be ≥ 10 orders of magnitude for some ocean regions; Hamilton et al. 2019) and an increasing appreciation of the role of atmospheric processing in enhancing aerosol nutrient solubility during transport (Longo et al. 2016, Stockdale et al. 2016) make data acquisition of representative field observations a challenge that needs to be addressed.

Nitrogen is a core element for sustaining biological systems and functions, but it is found mainly in its highly stable elemental form (N_2), which is not bioavailable. However, through biological nitrogen fixation by diazotrophs, N_2 enters the ocean biosphere and provides the largest source of bioavailable new nitrogen in the open oceans (Capone et al. 1997, Jickells et al. 2017, La Roche & Breitbarth 2005). A smaller amount of reactive nitrogen (hereafter referred to simply as nitrogen) that is present is bioavailable (Altieri et al. 2021 and references therein) and strongly

associated with anthropogenic sources (Jickells et al. 2017). Owing to the significant amount of literature reviewing nitrogen supply, further discussion here is limited.

Phosphorus is another vital nutrient for supporting life. Because heavy particles fall below the ocean's mixed layer, only phosphate may be relevant for marine biota, although observations remain limited (Baker et al. 2006, Mahowald et al. 2008). Oceanic regions considered colimited by phosphate include the western North Atlantic and eastern Mediterranean Sea (Moore et al. 2013). Additionally, the North Pacific Subtropical Gyre can be phosphate limited at times, oscillating with iron limitation (Letelier et al. 2019). In addition to dust, wildfires and primary biogenic particles are likely to be important sources of phosphate to much of the open ocean (Barkley et al. 2019, Myriokefalitakis et al. 2016). The diversity of sources partially explains why high phosphate concentrations are observed outside of major dust plumes from the Northern Hemisphere dust belt and Patagonia (**Figure 1**).

Due to iron's potential to significantly modulate the marine carbon cycle (Cassar et al. 2007, Martin 1990), there have been considerable efforts to understand the iron cycle and its role in supporting both phytoplanktonic NPP in high-nutrient, low-chlorophyll (HNLC) waters and diazotrophic uptake of atmospheric N₂ at tropical latitudes. Numerous studies, including in situ iron fertilization experiments, ocean surveys, and modeling, have revealed that iron limitation of phytoplankton is the primary factor regulating NPP levels in the upwelling region of the equatorial Pacific, the subarctic Pacific and Atlantic, and the Southern Ocean (de Baar et al. 2005, Moore et al. 2013). Here, we explore in detail the role of the iron supply from nondust sources in marine biogeochemical cycles.

The factors that promote mineral dissolution processes, such as increasing atmospheric acidity, the presence of organic ligands, sunlight, high surface-area-to-volume particle ratios, and elevated temperatures (e.g., Lasaga et al. 1994), represent one of the largest sources of uncertainty in state-of-the-art model simulations. During long-range atmospheric transport, strong acids, such as sulfuric acid (H₂SO₄) and nitric acid (HNO₃), coat phosphorus- and iron-bearing aerosols and work to liberate them into a soluble (bioavailable) form (Herbert et al. 2018, Myriokefalitakis et al. 2016, Nenes et al. 2011, Shi et al. 2011). This phenomenon also enriches particles with nitrogen, as already observed for dust (Geng et al. 2009). Such well-mixed deposits produce a favorable cocktail of chemical elements vital for biota (nitrogen, phosphorus, and iron) being supplied to the surface ocean. Studies have also suggested that the atmospheric dissolution of mineral iron is significantly enhanced in the presence of organic compounds such as oxalic acid, which may result in a >75% iron solubility enhancement compared with acid processing alone (Ito 2015, Ito & Shi 2016, Johnson & Meskhidze 2013, Myriokefalitakis et al. 2015) (for more discussion, see the section titled The Organic Nutrient Fraction). Recent modeling has estimated that atmospheric processing creates an additional 0.56 ± 0.29 Tg of soluble iron per year (Myriokefalitakis et al. 2018) and 0.030 Gg of soluble phosphorus per year (Herbert et al. 2018).

Postdeposition processes also affect atmospheric iron and phosphorus bioavailability. It is well understood that multiple factors operate in tandem to determine the fate of atmospheric dissolved iron concentrations, such as iron dissolution kinetics, binding ligands, scavenging, and biotic uptake (Baker & Croot 2010, Boyd & Ellwood 2010, Bressac & Guieu 2013, Fishwick et al. 2014). Seasonal variations in the ocean mixed layer affect dissolved iron concentrations following deposition, with little change during periods of deep mixed layers and the detrainment of aerosol iron below the shoaling springtime mixed layer. Depending on the nature and quantity of dissolved organic matter present at the time of deposition, the same dust or simulated flux can provoke either iron scavenging (Wagener et al. 2010) or dissolution (Bressac & Guieu 2013, Wagener et al. 2008). Postdeposition processes for atmospheric phosphorus are linked to the amount of

Dust belt:

a latitudinal band that includes the primary dust source regions of North Africa, the Arabian Peninsula, and central Asia

High-nutrient, low-chlorophyll (HNLC) waters:

waters in which nitrogen and phosphorus are present in excess compared with biological requirements but chlorophyll levels are atypically low

Oligotrophic:

depleted in nutrients and exhibiting low surface chlorophyll; typically refers to regions where chlorophyll *a* concentrations are $<0.1 \mu\text{g L}^{-1}$

iron oxides present. In abiotic conditions, a transient release of phosphate is usually observed in seawater, rapidly followed by a strong concentration decrease due to adsorption onto iron oxides (Louis et al. 2015, 2018), confirming that interactions between phosphate and iron oxyhydroxides exert a key control on phosphate availability in the environment (Chitrakar et al. 2006). Still, the role of dissolved organic matter via dust-aggregation processes could prevent those interactions in some cases (Louis et al. 2015). Cellular iron quotas vary both spatially and seasonally (Boyd et al. 2012, 2015; Twining & Baines 2013; Twining et al. 2020) and thus play a crucial role in linking changing aerosol iron supply to the response of phytoplankton productivity, adding yet another layer of complexity to understanding the importance of atmospheric deposition. While new modeling efforts start to account for the scavenging role of dust particles when estimating dissolved iron concentrations (Ye & Völker 2017), more work is required to account for other aerosol iron phases, which may have distinct sizes, dissolution kinetics, reactivity, and organic phases.

Although complex processes are at play in determining the fate of atmospheric nutrients, some biological response patterns are evidenced by aerosol addition experiments using seawater from different regions of the world. **Figure 2** presents a compilation of those data ($n = 70$), reporting a relative change (maximum change shown) in autotroph biomass following aerosol addition. Although such experiments are not fully representative of the impact of atmospheric nutrient deposition to the ocean (Guieu et al. 2014a), autotroph biomass is the parameter for which we have the most data available. Although the average experimental outcome is in favor of an increase ($\sim+80\%$) in chlorophyll *a* following artificial addition, in many cases no response or a negative impact was reported when the aerosol deposition did not relieve ongoing nutrient limitation (Guieu et al. 2010), reinforced the initial metabolic balance toward heterotrophs (Gazeau et al. 2020, Marañón et al. 2010), or induced a toxic effect (Paytan et al. 2009, Zhang et al. 2019).

These disparities in biological response reveal that the bioavailability of chemical elements carried by aerosols depends on a complex set of processes. Governing parameters include the emission source and mixing processes that occurred during transport, the type of deposition (dry or wet), and the biogeochemical state of the seawater receiving aerosol deposition. Such experiments, which are conducted mostly over a short period of time, show that the impact (positive or negative) of atmospheric deposition on the biomass of autotrophs is, when it exists, rapid (a few days). To date, these experiments have been conducted mainly in oligotrophic environments (**Supplemental Table 1**) and resulted in modest and short-term changes of total biomass. Overall, aerosols from either anthropogenic or mixed sources stimulated chlorophyll *a* $\sim 50\%$ more than dust aerosol alone (dust alone, $+70\%$; anthropogenic/mixed, $+108\%$). Additional experiments are required to cover the vast area of the ocean where this type of data remains lacking.

THE COMPLEX INTERPLAY OF DUST AND FIRE AEROSOL SOURCES

Multimodel estimates of global dust emissions fall between 735 and 8,186 Tg y^{-1} (median 2,467 Tg y^{-1}), with the highest values simulated by a model that resolves particle size distributions above 20 μm and up to 63 μm (Wu et al. 2020). Approximately 90% of all dust emissions are located in the Northern Hemisphere dust belt (Ginoux et al. 2012) but are highly episodic, resulting in a large proportion of dust aerosol deposition to ocean basins (30–90%) occurring over only ~ 18 days per year (5% of the year) (Mahowald et al. 2009). Dust is a significant source of mineral nutrients (**Figure 3**), and how far deposition sustains NPP is a question asked for many basins (Fung et al. 2000, Guieu et al. 2019, Martin et al. 1991). Mineral dust phosphorus and iron tend to be relatively insoluble compared with other sources, however (**Figure 3a**), and in the case of iron, while dust represents up to 95% of the global atmospheric budget (Mahowald et al. 2009), aluminosilicate and iron-oxide minerals with extremely insoluble crystalline lattices dominate emissions ($<1\%$ solubility; Journet et al. 2008). The compositions of soils from which dust originates are

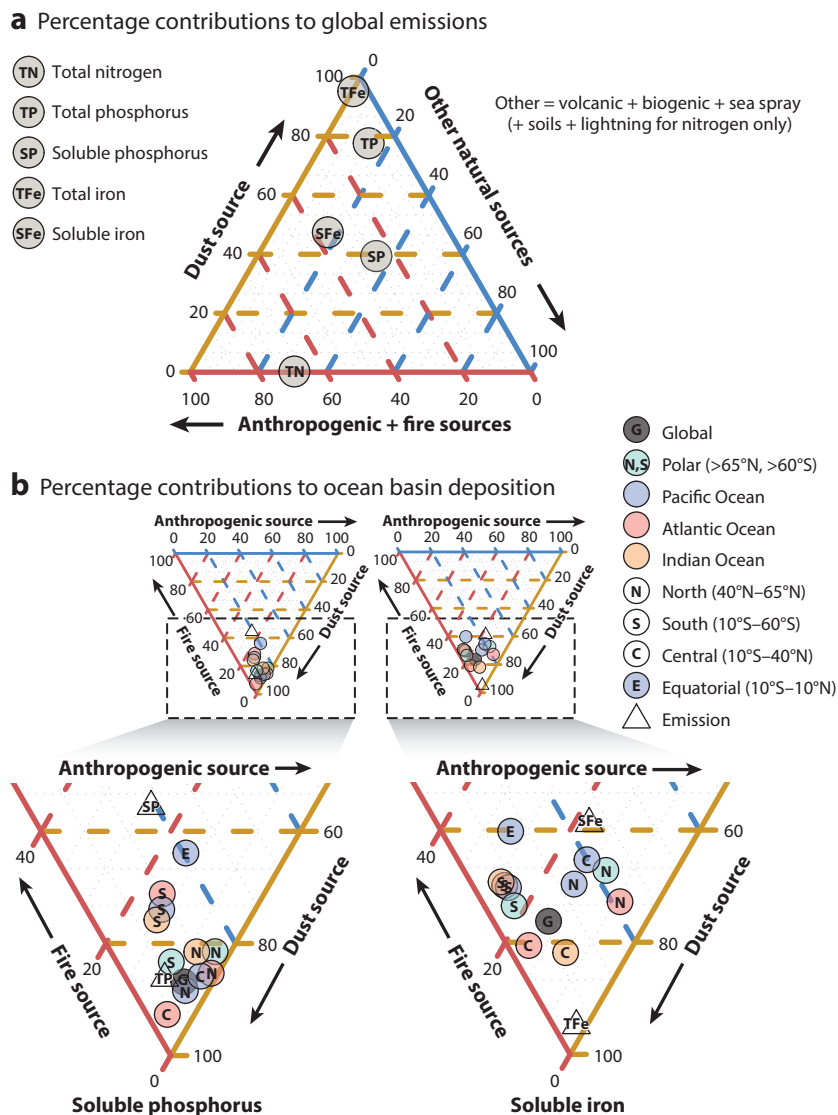


Figure 3

Percentage contributions of (a) different aeolian sources to global atmospheric nutrient emissions and (b) different aeolian sources to the atmospheric deposition flux to different ocean basins. Emission data in panel a are from Kanakidou et al. (2018) and iron modeling. Deposition data in panel b are from modeling: Phosphorus data are from Myriokefalitakis et al. (2020), and iron data are from Myriokefalitakis et al. (2020) and separate modeling performed for this review (see **Supplemental Table 2**). In panel b, the equatorial area is a high-nutrient, low-chlorophyll subregion in the central Pacific.

Supplemental Material >

In situ and lidar remote sensing suggests the presence of mineral dust particles in wildfire smoke plumes (Kavouras et al. 2012, Nisantzi et al. 2014, Schlosser et al. 2017), and increased dust emissions from postfire burned landscapes have been reported (Dukes et al. 2018, Jeanneau et al. 2019, Wagenbrenner et al. 2017, Whicker et al. 2006). However, the total fraction of dust (and hence phosphorus and iron) emissions caused by fires has not yet been quantified. The average

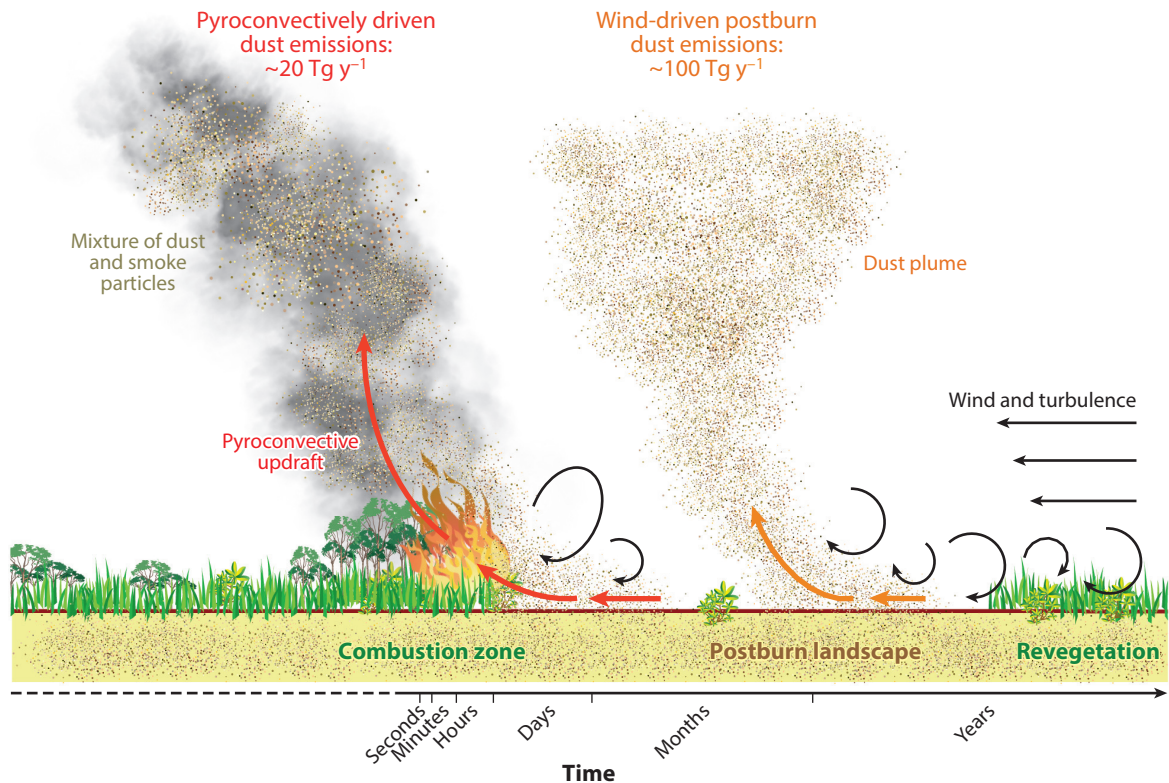


Figure 4

Properties and estimated magnitudes of dust emissions during and after a fire as a function of time starting with an active fire. For details on the estimated global annual dust fluxes, see the sidebar titled *The Interface Between Fires and Dust* along with the **Supplemental Material** section titled *Methods*.

Supplemental Material >

iron:aluminum ratio compiled from 30 years' worth of field campaigns investigating aerosol composition within (mainly tropical) biomass-burning regions ($n = 17$; see **Supplemental Tables 3 and 4** and **Supplemental Figure 1**) is $\sim 0.6:1$. Fires are likely enriched in iron above the global mean crustal ratio (0.44:1; McLennan 2001) by approximately one-third ($\sim 36\%$), in agreement with previous studies suggesting that the majority of iron in grassland and forest fires comes from the surrounding soils, either directly or via resuspended particles previously deposited on vegetation (e.g., Gaudichet et al. 1995, Maenhaut et al. 1996, Paris et al. 2010). Compared with ordinary dust storms, fire-driven (pyroconvective) dust emission allows for (a) increasing emissions of larger particles, (b) entrainment at higher altitudes, and, if the dust is entrained in the free troposphere or above, (c) longer atmospheric travel distances and associated processing; for example, smoke from the 2020 Australian megafire circumnavigated the Southern Hemisphere (Khaykin et al. 2020). In addition to the heat generated in fires determining the strength of pyroconvective upwinds, high temperatures can alter soil morphology and other properties, such as mineralogy, texture, porosity, particle size distribution, and water capacity (Atanassova & Doerr 2011, McNabb & Swanson 1990, Pérez-Cabello et al. 2006). The coupling of fires and dust emission processes likely constitutes a large source of uncertainty for marine biogeochemical studies; a first estimate of enhanced global dust and related iron aerosol emission fluxes, both during and following biomass-burning events, is provided in the sidebar titled *The Interface Between Fires and Dust*.

THE INTERFACE BETWEEN FIRES AND DUST

In-Plume Dust Entrainment

In an idealized model study, Wagner et al. (2018) investigated the impact of different agriculture-related fires on near-surface wind patterns and found aerodynamic conditions suitable for dust emission in the vicinity of such fires. In later work, the simulated fire-modulated winds were coupled with two different dust emission parameterizations to obtain first estimates of the effectiveness of pyroconvectively driven dust emissions (R. Wagner, K. Schepanski & M. Klose, manuscript in review). Depending on the model setup, this latter study found fire-driven dust emission fluxes of 1.0–5.0 g m⁻² h⁻¹, which would, if scaled up globally, account for up to 20 Tg y⁻¹. With respect to total global dust emissions—estimated between 700 and 3,600 Tg y⁻¹ in models with comparable particle sizes (0.06–20 μm) (Wu et al. 2020)—pyroconvectively driven dust emission could therefore contribute an additional 3–14%, especially in regions outside the dust belt. Assuming that the dust iron fraction is 3.5% and that 64% of fire iron is dust sourced gives iron emissions (<20-μm particle size) of 1.1 Tg y⁻¹ from fires, which is the same as a previous estimate by Luo et al. (2008).

The Postburn Landscape

The strength and duration of postfire dust emissions can vary significantly depending on the geographical location, meteorology, and revegetation period. Results from several studies reflecting geographical diversity point toward a large variability of enhanced dust fluxes between individual sites (Dukes et al. 2018, Jeanneau et al. 2019, Whicker et al. 2006). Using their averaged results as a proxy for postburn landscapes and assuming that the periods without vegetation permit wind erosion (for months to a year) suggests that such postfire emissions could potentially contribute on the order of magnitude of 100 Tg y⁻¹ of soil dust emissions, with a possible uncertainty interval of the same order of magnitude. However, postfire sources might already be at least partly considered in global estimates of dust emission fluxes.

Nitrogen emissions from biomass burning are well characterized in the literature (e.g., Andrea 2019), but estimates of other nutrients are currently missing. Overall, fire iron and phosphorus each contribute <1% of the total mass emitted in fires (Reid et al. 2005). Mahowald et al. (2005) and Luo et al. (2008) used Amazonian biomass-burning observations of phosphorus and iron, respectively, to estimate emission ratios relative to black carbon. As black carbon is a product of combustion and a core component in atmospheric models, this approach provided a convenient methodology to estimate global phosphorus and iron emissions from fires (Mahowald et al. 2008; Myriokefalitakis et al. 2016, 2018). Here, we extend this analysis beyond the Amazonian region and find a mean iron:black carbon ratio of 0.30:1–0.41:1 and a mean phosphorus:black carbon ratio of 0.016:1–0.12:1, suggesting that iron is being emitted at at least double the rate of phosphorus in fires (**Supplemental Tables 3 and 4**). Particle size–segregated observations are more limited but suggest that coarse particles of phosphorus and iron are emitted at significantly higher ratios (mean across studies of 0.026:1–0.25:1 and 0.74:1–0.80:1, respectively) than fine particles (mean across studies of 0.0013:1–0.010:1 and 0.019:1–0.032:1, respectively). Lower ratios were derived using observational data to calculate linear regression coefficients (**Supplemental Figures 2 and 3**), while higher values are the mean across reported literature values from only studies conducted near fire activity or reporting dry (biomass-burning) season values (**Supplemental Table 3**). The lower phosphorus:black carbon ratios are similar to those reported by Mahowald et al. (2005). Likewise, the lower fine iron:black carbon ratio is similar to ratios reported by Luo et al. (2008), but the lower coarse-mode ratio is a little over half their value of 1.4:1, which is based on fewer observational data than are used here. As dust emissions are mostly coarse particles, while combustion emissions are generally fine particles, this suggests a major presence of iron and phosphate from dust in fire plumes. Forest and/or less energetic (smoldering) fires may also release more

Supplemental Material >

Coarse: having a particle diameter larger than 1 or 2 μm

Fine: having a particle diameter less than 1 or 2 μm

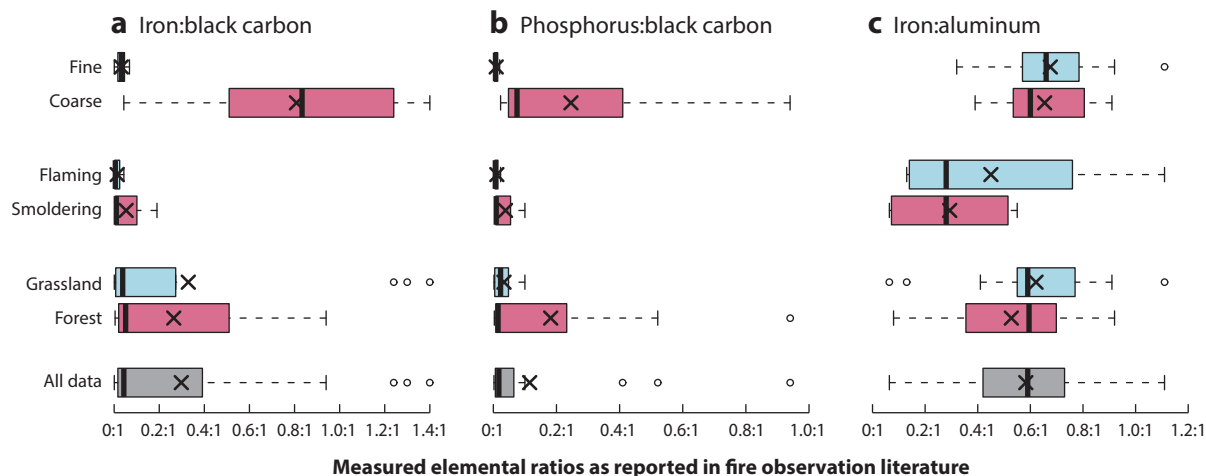


Figure 5

Range in observed (a) iron:black carbon, (b) phosphorus:black carbon, and (c) iron:aluminum ratios in fire aerosol as reported in the studies listed in **Supplemental Table 3**. X's indicate means.

Supplemental Material >

nutrients compared with grassland and/or intense (flaming) fires (**Figure 5**). However, observations comparing the nutrient content in aerosols from flaming and smoldering fires are scarce. Additional study is necessary to understand what fire characteristics determine their potential for nutrient delivery.

An early study by Guieu et al. (2005) estimated that at the global scale, soluble iron deposition from fires was $\leq 10\%$ of that from dust. Increased observations and process understanding led to an updated estimate of $\sim 20\%$ (18.4–22.5%; see **Supplemental Table 2**). Regionally and during the burning (dry and warm) season, this contribution can be higher; for example, Southern Hemisphere soluble atmospheric iron and phosphorus deposition from fires and dust may be similar (Barkley et al. 2019, Hamilton et al. 2020b). A linkage between fire emission and enhanced aerosol solubility has been suggested downwind of burning regions, but this mechanism remains unclear (Mahowald et al. 2018, Paris et al. 2010, Perron et al. 2020). In the case of iron, studies have estimated solubility from fire sources to be between 2% and 46%. The lowest solubilities were observed from southern European and western African sources (2%) (Guieu et al. 2005, Paris et al. 2010), midrange solubilities were observed from Australian sources (18%) (Bowie et al. 2009) and based on wood composition (10–15%) (Rathod et al. 2020), and the highest solubilities came from a controlled-burn laboratory study in the southeastern United States (46%) (Oakes et al. 2012).

The large range in reported fire iron solubilities has led to differing representations in models. Some investigations have proposed that fire iron solubility is 0% at emission, with acidic and organic compounds coemitted in fires significantly enhancing the solubility of both fire and dust iron sources during the transport of the smoke plume (Ito 2015). Others have chosen to apply a higher initial fractional solubility to fire iron (compared with dust sources), e.g., 33% and 4% for fine and coarse particle emissions, respectively (Hamilton et al. 2019). The postulate of fire plumes from Australian sources being a nutrient source to downwind oceanic regions was recently supported by field measurements of high aerosol iron solubility in concurrence with intrinsic or remotely sensed indications of the presence of aerosols from fires in samples collected at several places across Australia (Perron et al. 2020, Strzelec et al. 2020, Winton et al. 2016). When Ito et al. (2020a) implemented such field observations in an inverse model, they estimated that the minor

Smoldering:

characterized by an often persistent, low-temperature, flameless burning that produces significant volumes of smoke

Flaming:

characterized by a higher-temperature burning with flames that produce less smoke

source of iron from Australian bushfires represented the dominant source of soluble iron (up to 82% regionally) due to its higher solubility compared with iron from mineral dust. We further explore the role of Australian (wild)fires in Southern Ocean biogeochemical cycles in a case study below (see the section titled Australia: A Major Nutrient Source to Southern Hemisphere Oceans).

VOLCANIC AEROSOL IMPACTS ON MARINE NUTRIENT SUPPLY

Volcanic eruptions release large volumes of volcanic ash and aerosols into the atmosphere, making them an important natural nutrient source to the open ocean, especially on local to regional scales. The physicochemical properties and depositional patterns of volcanic aerosols differ from those of mineral dust, wildfires, or anthropogenic sources (Langmann 2013). Volcanic ash is a size class of fragmented particles with diameters from submicron to a few millimeters; such a large particle size range affects settling velocities and hence the nutrient flux to receiving water columns. The chemical compositions, surface salt coatings, and particle size distributions of volcanic ashes vary widely, as does the array of nutrients (Duggen et al. 2007, Olgun et al. 2013) and trace metals (Hoffmann et al. 2012, Mahowald et al. 2018) released.

The volcanic ash supply to marine environments is as high as 100 g m^{-2} in the vicinity of the volcano, decreasing exponentially to values of $0.1\text{--}0.3 \text{ g m}^{-2}$ several hundred kilometers away in open ocean regions (Olgun et al. 2013). The most important volcanic ash deposition regions are the equatorial eastern Pacific, which receives ash from the Central American Volcanic Arc; the northwestern Pacific, which receives ash from the Kamchatka Peninsula and Aleutian Islands; and the southwestern Pacific, which receives ash from the South American volcanic arcs (**Figure 6**). Estimates based on marine sediment core data show that $128\text{--}221 \times 10^{15} \text{ g}$ of volcanic ash has been deposited into the Pacific (covering $\sim 70\%$ HNLC regions) during the last millennium. Remote volcanic hot spots, such as Iceland and Hawaii, are also important nutrient sources to the North Atlantic and North Pacific (**Figure 6**).

In addition to volcanic ammonium-bearing clinopyroxene minerals, both intense lightning within volcanic eruption plumes and atmospheric processing are important sources of nitrogen-bearing compounds on ash surfaces. The mineral composition of volcanic ashes constitutes

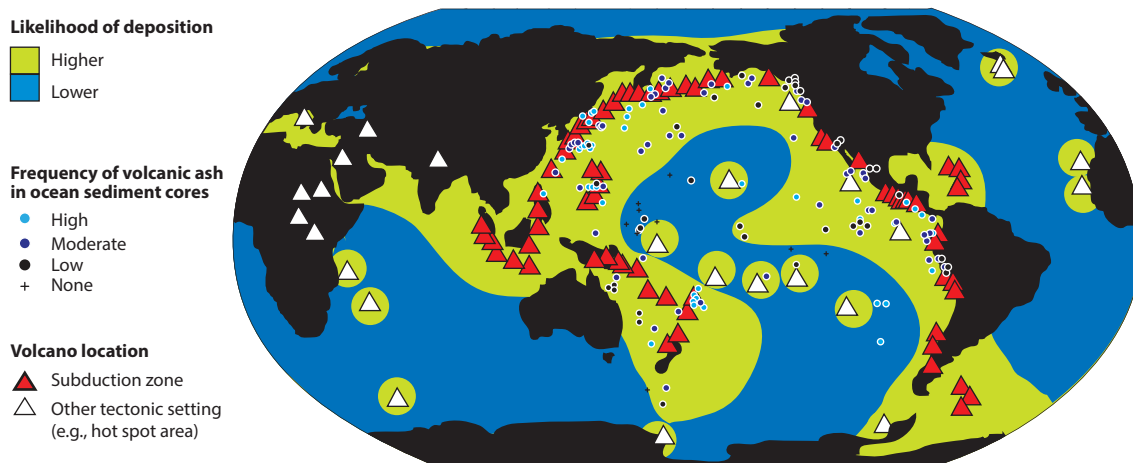


Figure 6

Global distribution of volcanoes and offshore ash deposition areas. The regions with a higher likelihood of ash deposition (green) are defined based on the low-altitude wind direction and the frequency of volcanic ash layers found in oceanic sediment cores during the Quaternary (Straub & Schmincke 1998). Figure adapted from Olgun et al. (2011).

45–75 wt% silica and 1.0–11.0 wt% iron, depending mainly on the chemistry of the lava and eruption type. The iron solubility of volcanic ash varies significantly, with the highest solubilities measured in acidic (pH 1–5) solutions (22%) and lower solubilities measured in buffered seawater (0.001–1.8%) (Duggen et al. 2010). There is no positive correlation between the iron content of ashes and the amount of iron released into the seawater (57–314 nmol of iron released per gram of ash; Olgun et al. 2011), and Duggen et al. (2010) suggested that the most likely source for the rapid iron release is the soluble surface salt coatings in the form of iron-bearing halides that are formed within the eruption plume.

ANTHROPOCENE PERTURBATIONS TO AEROSOL NUTRIENT SOURCES

Increased industrial, transport, mining, and agricultural activities provide new nutrient emission sources to the atmosphere, imposing a significant increasing trend in nutrient (and toxicant) deposition to marine ecosystems (Hamilton et al. 2020b, Ito 2015, Jickells et al. 2017, Luo et al. 2008, Matsui et al. 2018, Myriokefalitakis et al. 2020). Additionally, natural emissions are affected by human activity through anthropogenic land use and climate changes. For example, since the Industrial Revolution, dust emissions may have doubled (Mahowald et al. 2010), while fire emissions may have halved (Hamilton et al. 2018). Overall, the hemispheric balance of aerosol nutrient deposition, and thus of NPP, has likely shifted positively toward the Northern Hemisphere since the Industrial Revolution (Hamilton et al. 2020a, Jickells et al. 2017, Myriokefalitakis et al. 2020).

Anthropogenic activity has introduced two new phosphorus sources: industrial combustion and fertilizer production and use. Global fossil fuel and biofuel combustion sources are estimated to release 43–45 Gg of phosphorus annually, assuming 50% solubility at emission would result in ~22 Gg of phosphate emitted (Mahowald et al. 2008, Myriokefalitakis et al. 2016). Fertilizer production–related emissions occur during phosphate rock processing, drying, and storage. Furthermore, some nitrogen and potassium fertilizers include a phosphate component (such as ammonium phosphate or potassium phosphate). The Food and Agriculture Organization of the United Nations predicted that between 2015 and 2020 worldwide pure phosphate fertilizer demand would increase by ~11% (from ~41 Tg to ~46 Tg), nitrogen fertilizer demand would increase by 8%, and potassium fertilizer demand would increase by 12% (FAO 2017). Phosphate emissions occurring either during production or from fields after the application of any phosphate-containing fertilizer can be mostly considered bioavailable due to their intended end use for plant uptake. This potentially considerable source of readily soluble phosphate from fertilizer is not currently represented in global models and thus should be investigated further, as demand is predicted to continue increasing in the future.

Several studies have tentatively quantified the fraction of the aerosol nutrient burden in the atmosphere that comes from anthropogenic sources (e.g., Jickells et al. 2017, Lamb et al. 2021, Matsui et al. 2018). In particular, the use of differences in nitrogen and iron isotope fractionation could aid in distinguishing human from natural sources *in situ* (Altieri et al. 2021, Conway et al. 2019), although additional fractionation associated with atmospheric chemistry during transport can also influence measured values. While anthropogenic aerosol is, in general, pervasive throughout the globe, some pristine aerosol regions may exist and are most likely to occur in summer over HNLC marine regions (Hamilton et al. 2014, Uetake et al. 2020). That HNLC marine regions are colocated with the atmospheric regions that are presently least affected by human activity suggests that future anthropogenic activity hot spots could impact biogeochemical cycles if they develop upwind of pristine regions (Hamilton et al. 2020a, Myriokefalitakis et al. 2020). Fu et al. (2016) examined results from nine Earth system models to predict that NPP will decrease owing

Isotope fractionation: physical, chemical, and biological processes that enrich one isotope relative to another in predictable ways, creating distinct source fingerprints

Pristine aerosol region: a region where the post-Industrial Revolution human influence on the aerosol state likely remains minimal

Levogluconan: an indicator of wood combustion derived from the pyrolysis of (hemi)cellulose molecules

to increased ocean stratification under future warming ocean conditions. Increased (decreased) anthropogenic nutrient fluxes may partially offset (enhance) such reductions (e.g., Wang et al. 2015); however, if human activity preferentially increases nitrogen and phosphate deposition, marine ecosystems may further shift toward iron or other micronutrient limitation (Letelier et al. 2019, Mahowald et al. 2018).

THE ORGANIC NUTRIENT FRACTION

Observations compiled by Kanakidou et al. (2012) suggest that ~35% of both aerosol nitrogen (3–90%) and phosphorus (20–83%) could be organic in nature, while modeling suggests a corresponding deposition flux fraction of ~20–25% for nitrogen (Kanakidou et al. 2016) and up to ~50% for phosphorus (Myriokefalitakis et al. 2016). Recent biogeochemistry model calculations showed that when organic nutrients are considered, substantial increases in nitrogen fixation were simulated in the tropical Pacific and Atlantic but were balanced by decreases elsewhere (up to ~40%) due to the additional nitrogen inputs through organics (Myriokefalitakis et al. 2020). Although the overall impact of atmospheric organic nutrient inputs to the ocean on marine NPP is generally estimated to be low on a global scale (~2.4%), stronger regional changes are calculated within the oligotrophic subtropical gyres, where the additional atmospheric nitrogen deposition can support extra production of up to 15–20% (Myriokefalitakis et al. 2020).

Atmospheric organic nitrogen has a strong anthropogenic component, while organic phosphorus is found mainly in natural phosphorus-bearing aerosols, such as bioaerosols (**Figure 3a**). The primary biogenic particles are leaf pieces, bacteria, fungi spores, and pollen released into the atmosphere either deliberately by biota or accidentally through entrainment by strong winds (Després et al. 2012, Jaenicke et al. 2007, Mahowald et al. 2008). Although these particles are poorly studied, most authors suggest that they have higher concentrations above high-productivity forests. For example, above the Amazon forest, estimates suggest that 30% of the <10- μ m particles are primary biogenic particles (Graham et al. 2003). Since most life forms have elevated phosphorus (Redfield ratios suggest ~0.5%) compared with crustal content (<0.1%), primary biogenic particles are thought to be an important source of phosphorus to the atmosphere, although much of this phosphorus is enclosed in large particles that fall close to the emission source (Brahney et al. 2015, Tipping et al. 2014). Biogenic particles are likely to contain mostly bioavailable phosphorus, and thus they may represent the most important source of soluble phosphorus to many ocean regions (Myriokefalitakis et al. 2016).

On the other hand, organic-bound iron is produced during transport when iron-containing aerosols undergo organic ligand-mediated dissolution processes [e.g., as Fe(II/III)-oxalate complexes]. Of the atmospheric organic ligands, oxalic acid is currently considered the most important species, and it is used as a proxy for organic ligand-mediated iron dissolution processes because it is thought to be the most abundant species in the atmosphere and is the most effective ligand in promoting iron solubilization through the formation of iron-oxalate complexes at the mineral's surface that polarize and weaken iron-oxygen bonds (e.g., Ramos et al. 2014). Oxalic acid is produced within the atmosphere by aqueous-phase photochemical processes, mainly in cloud droplets (e.g., Myriokefalitakis et al. 2011). Biogenic volatile organic compounds are the most important precursors, and owing to their strong source, intense photochemistry, and strong convective transport potential, high concentrations of oxalate (the deprotonated form of oxalic acid) are found in tropical regions (Myriokefalitakis et al. 2011). However, dicarboxylic acids in the atmosphere may also have various primary sources, including biomass burning, vehicular exhaust, and cooking emissions. Dicarboxylic acids show, nevertheless, a strong correlation with elemental carbon and levoglucosan (Cao et al. 2017, Cong et al. 2015), and high concentrations of oxalic acid

have been observed during the Amazonian burning season (Kundu et al. 2010). This suggests that biomass burning (rather than coal combustion or vehicular exhaust) could be an additional atmospheric source of oxalate (Schmidl et al. 2008, Yamasoe et al. 2000). Some studies postulated that high temperatures generated by fires may catalyze the transformation of insoluble iron oxides in soils into more labile forms in the presence of organic matter (Ito et al. 2018). Such modified soils are entrained into the atmosphere both during and after fires (see the sidebar titled The Interface Between Fires and Dust).

AUSTRALIA: A MAJOR NUTRIENT SOURCE TO SOUTHERN HEMISPHERE OCEANS

Australia is one of the largest arid regions in the Southern Hemisphere, along with Patagonia in South America and the Kalahari and Namib Deserts in southern Africa. The central Outback region of Australia is composed of large sandy deserts toward the west and arid geological basins (Lake Eyre and the Murray–Darling Basin) toward the east. The Australian atmospheric circulation is divided into three main aerial pathways, potentially irrigating: (a) the Indian Ocean, via the northwest dust path; (b) the Tasman Sea, Southern Ocean, and South Pacific, downwind from the southeast dust path; and (c) the Great Australian Bight, through a smaller atmospheric depression blowing southwestward across Western Australia's southern coast. Large dust storms frequently emphasize the uplift and transport processes of iron-bearing dust in Australia, with megatons of red soil particles being carried away to surrounding marine areas (Gabric et al. 2010, Mackie et al. 2008). Current modeling projections suggest that Australia accounts for 10% (4–30%) of dust deposited into the Southern Ocean, 7% (3–11%) of dust deposited into the Indian Ocean, and 68% (20–81%) of dust deposited into the South Pacific (Kok et al. 2021).

In addition to being a major dust source, southern Australia is frequently hit by devastating summer wildfires, as happened during the summers of 2002–2003, 2005–2006, 2006–2007, 2009, and 2012–2013 (For. Fire Manag. Vic. 2021), as well as during 2018–2019 in Tasmania (Lucas & Harris 2021). Recently, the 2019–2020 Australian megafires had an unprecedented impact on Australia's vegetation, burning no less than 21% of the country's temperate and broadleaf forests (Boer et al. 2020). Fire-induced pyrocumulonimbus clouds associated with this natural disaster spread aerosol across the whole Southern Hemisphere, leading to a major and long-lasting (months-long) perturbation of the hemisphere's atmospheric composition, including the stratosphere. For comparison, the perturbation resulting from the magnitude, elevation, and long-range transport of the 2020 Australian fire plume was as large as any atmospheric perturbation following a volcanic eruption since the 1991 Pinatubo eruption (Khaykin et al. 2020).

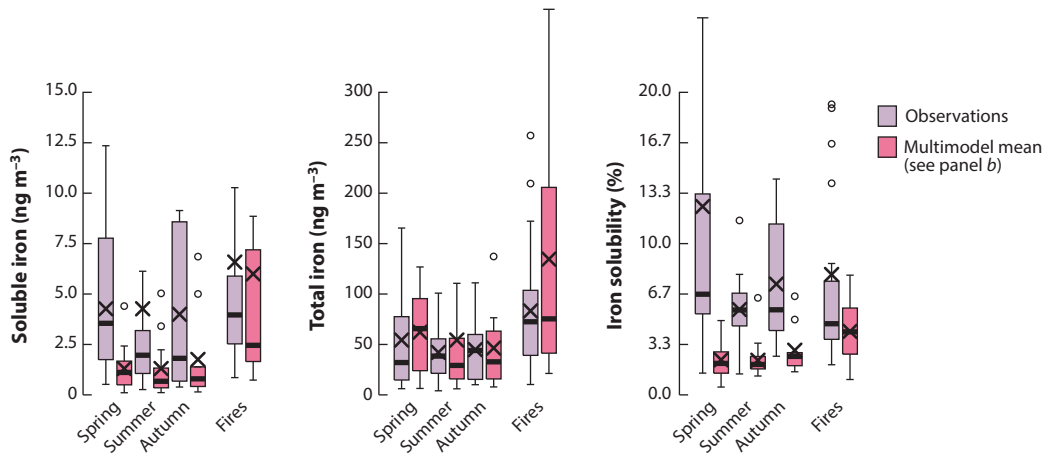
Recent time series observations (2016–2020) from samples collected at Mount Wellington in Tasmania (42.9°S, 147.2°E) reveal the aeolian transport of nutrients from Australia southward and into the Southern Ocean. **Figure 7a** compares the total and soluble iron measurements with results from two atmospheric iron models: Integrated Massively Parallel Atmospheric Chemical Transport (IMPACT) (Ito et al. 2021) and Mechanism of Intermediate Complexity for Modeling Iron (MIMI) (Hamilton et al. 2020b) (see the **Supplemental Material** section titled Methods). The four-year field observations show that, during burning periods, atmospheric iron loading is significantly higher than it is during nonfire days regardless of the season. This further suggests that wildfires are a nonnegligible source of iron to Australian atmospheric transport pathways. While biomass contains small amounts of iron, this raises the question of which mechanism leads fire emissions to entrain a significant number of iron-bearing particles within their plumes (**Figures 4** and **5**; see also the sidebar titled The Interface Between Fires and Dust).

Dust alone requires extensive atmospheric processing to reach the high aerosol iron solubility measured in field observations, which often exceeds 10% over much of the Southern Hemisphere

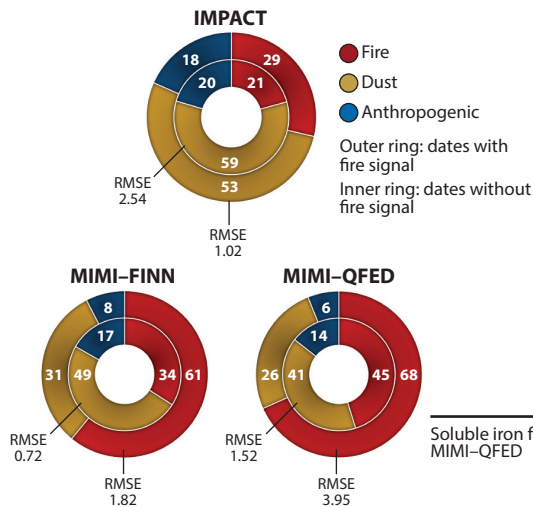
Supplemental Material >

(Baker et al. 2013, Perron et al. 2020, Winton et al. 2015). Iron modeling currently includes dust, anthropogenic combustion, and fire sources of iron (Myriokefalitakis et al. 2018). Comparison of ensemble modeling with Mount Wellington observations suggests fidelity in representing the total mass of iron emitted from Australia (Figure 7a). However, while the observed soluble iron range on fire days (defined as days with an intrinsic levoglucosan measurement of $>10 \text{ ng m}^{-3}$) is captured, the median (2.5 ng m^{-3}) is lower than that observed (4.0 ng m^{-3}). Furthermore, modeling significantly underestimates median iron solubility for nonfire days (observed, 5.9%; IMPACT, 1.2%; MIMI, 3.1–3.6%), suggesting that either (a) there is a currently unaccounted-for

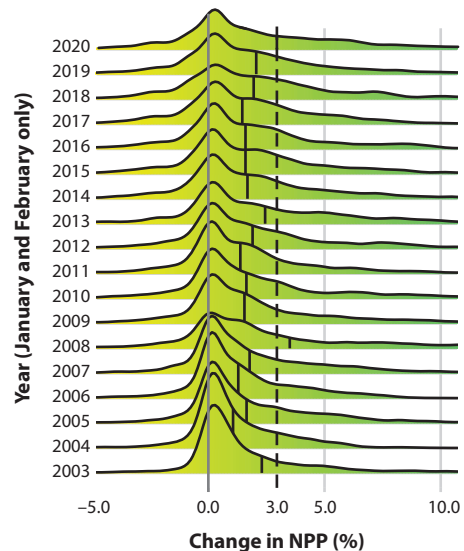
a Seasonal observations and modeling at Mount Wellington



b Modeled contributions of sources of soluble iron at Mount Wellington



c Changes in NPP in the Southern Ocean due to soluble iron deposition from fires



(Caption appears on following page)

Figure 7 (Figure appears on preceding page)

Potential impact of wildfires on marine biogeochemistry. (a) Seasonal observations and multimodel estimates of the mean concentration of soluble and total iron and aerosol iron solubility at Mount Wellington. X's indicate means. Fire-impacted data are defined when measurements of levoglucosan concentration in aerosol exceed 10 ng m^{-3} , a threshold that was chosen to exclude residual levoglucosan levels (Bhattarai et al. 2019) and ensures the sole selection of samples that display a distinct fire signal. (b) Fractional contribution of each aeolian source to the soluble iron loading at Mount Wellington, as predicted by IMPACT (Ito et al. 2021) and MIMI (Hamilton et al. 2020b) model simulations. The outer rings show the source contributions (percent) for dates when a fire signal was observed, and the inner rings show the source contributions (percent) for nonfire dates, according to levoglucosan measurements in the associated aerosol samples. (c) PISCES modeled annual percentage changes in depth-integrated NPP in the Southern Ocean ($30\text{--}65^\circ\text{S}$) based on MIMI-QFED soluble iron deposition during the Australian fire season (January and February). In each year, the black vertical solid line indicates the mean for that year. Across all years, the vertical black dashed line indicates the 2020 mean value, and the gray solid line indicates zero. Abbreviations: FINN, Fire Inventory from NCAR; IMPACT, Integrated Massively Parallel Atmospheric Chemical Transport; MIMI, Mechanism of Intermediate Complexity for Modeling Iron; NPP, net primary productivity; PISCES, Pelagic Interactions Scheme for Carbon and Ecosystem Studies; QFED, Quick Fire Emissions Dataset; RMSE, root mean square error.

(and important) atmospheric source of highly soluble iron emitted on these days or (b) processing of dust iron happens more quickly than currently realized under pristine conditions.

The contribution of each source to soluble iron concentrations differs between the two models (**Figure 7b**): IMPACT emphasizes dust, while MIMI emphasizes fires. The increased contribution of fires to soluble iron concentrations on fire days is also higher in MIMI than in IMPACT (51–79% increase versus 38%). Because near-future predictions warn of an increasing occurrence of conditions prone to the ignition of megafires in temperate regions of Australia (Di Virgilio et al. 2019, Dowdy et al. 2019), more constraints on the properties of fire-sourced iron, including its pyrogenic fraction, are needed.

We quantified the impact of the 2020 Australian megafires on ocean biogeochemistry using the Pelagic Interactions Scheme for Carbon and Ecosystem Studies (PISCES) model (Aumont et al. 2015) and compared it with the impact in previous years (**Figure 7c**). To isolate fire impacts, we ran the model twice (see the **Supplemental Material** section titled Methods), once with and once without fire iron deposition, and analyzed the difference between them for January and February (Australian peak fire activity). Model soluble iron from fire was predicted using daily Quick Fire Emissions Dataset (QFED) emissions, as this represented the maximum Australian emission estimate and also simulated the median soluble iron concentrations closest to the observations (observations, 4.0 ng m^{-3} ; IMPACT, 0.9 ng m^{-3} ; MIMI–Fire Inventory from NCAR (FINN), 2.4 ng m^{-3} ; MIMI–QFED, 4.5 ng m^{-3}). Large variability in the fire activity in different years increases Southern Ocean ($30\text{--}65^\circ\text{S}$) NPP between 1.1% and 3.5%, with the second-largest increase, 3.0%, occurring in 2020. As fires also represent a large source of nitrogen and phosphate (**Figure 3a**), 3% additional NPP may be a conservative estimate of the potential marine stimulation following atmospheric deposition of fire aerosol. Earlier modeling work showed that the combined addition of nitrogen and iron (as occurs in fire plumes) induces larger NPP globally than a single element supply would (Krishnamurthy et al. 2009).

In these experiments, fire deposition of soluble iron has a clear overall positive impact on NPP in subarctic and Southern Ocean HNLC regions (**Figure 8**). Depending on the year, fires increased annual global NPP up to 0.7% [Southern Ocean, 0.7–1.3%; central Pacific ($30^\circ\text{S}\text{--}30^\circ\text{N}$), $-0.3\text{--}1.2\%$; North Pacific ($45\text{--}65^\circ\text{N}$), $0.1\text{--}1.3\%$]. In some regions, such as the equatorial Pacific, NPP increases are balanced by decreases downstream, a result also seen in other studies that may be linked to macronutrient decreases downstream from where iron fertilization occurs (Hamilton et al. 2020a, Ito et al. 2020b, Tagliabue et al. 2008). Improved understanding of how variability in aerosol nutrient supply, over different timescales, impacts ocean biogeochemistry requires a holistic multidisciplinary approach, including consideration of the physicochemical properties of different nutrient aerosol sources, interactions during atmospheric transport that

Supplemental Material >

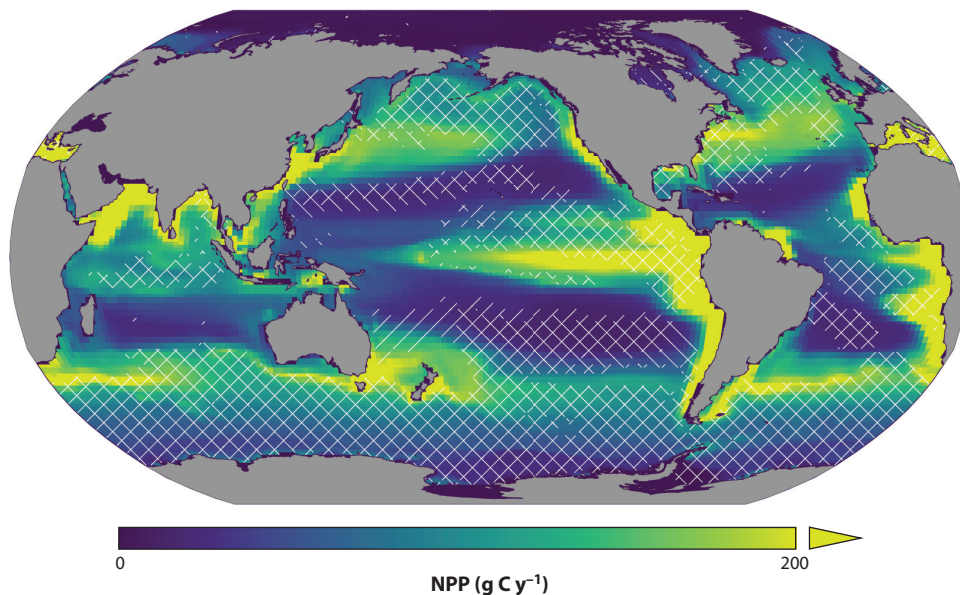


Figure 8

Annual mean (2003–2020) depth-integrated marine NPP. White lines indicate where soluble iron deposition from fires increased productivity. Increases in NPP from different fire emission data sets are indicated by the orientation of the line (45°, QFED; -45°, FINN); the absence of a line indicates a decrease in NPP. Abbreviations: FINN, Fire Inventory from NCAR; NPP, net primary productivity; QFED, Quick Fire Emissions Dataset.

alter bioavailability, mixing of aerosol nutrients from varied sources, and the multiple processes operating in the surface mixed layer after deposition.

SUMMARY POINTS

1. Major nutrient sources include deserts and soils, wildfires, volcanoes, biogenic particles, and industrial or vehicular pollution. Sources of nitrogen are strongly linked to human activity, while phosphate and soluble iron have considerable natural sources.
2. Northern Hemisphere ocean nutrient fluxes are dominated by mineral dust sources, with an additional anthropogenic source at (sub)polar latitudes. In the equatorial Pacific and Southern Hemisphere oceans, fires are likely to be important.
3. Two-thirds of the iron in fires could be associated with dust particles entrained within smoke plumes, although more work is needed to quantify this contribution. Additionally, fires transform the landscape (soils and vegetation), creating a legacy of secondary impacts that alter the nutrient aerosol supply until the ecosystem recovers.
4. In situ aerosol addition experiments suggest that atmospheric deposition favors an increase (~80%) in chlorophyll *a*. However, in many experiments no response was recorded, and occasionally aerosols act as a pollutant that decreases chlorophyll *a*. The characteristics of the receiving body of water, including its biota, are thus crucial to understanding the impacts of changes to aerosol nutrient delivery.

5. At the global annual mean, modeling suggests that fires have a net positive impact on net primary productivity (NPP) (up to a 0.7% increase depending on year). Regional increases can be higher (e.g., up to 1.3% in the Southern Ocean) and peak during the burning season (e.g., the 2020 January–February Australian megafires could have increased Southern Ocean NPP up to 3%).
6. A significant nonfire source of soluble iron reaching Tasmania or a mechanism increasing iron solubility may be missing from the current understanding and atmospheric simulations of the Southern Hemisphere iron cycle.

FUTURE ISSUES

1. What are the mechanisms by which aerosol nutrients are distributed to oceans under different climate regimes?
2. How do regional land use and climate change alter dust and (wild)fire activity (both historically and in the future) and their roles in global biogeochemical cycles?
3. What field observations can aid in linking aerosol sources to observed characteristics? Some suggestions include the following: Isotopes show promise in quantifying human versus natural source contributions within mixed air masses, but targeted sampling of emissions from fires, forests, volcanoes, urban environments, deserts, and mining operations is essential; time series stations can quantify natural variability and the impact of long-term anthropogenic surface disturbances as well as aid in extreme event attribution studies; aircraft measurements taken over marine regions complement current ship-based observations to build a profile of the distribution and changing properties of aerosol nutrients over their atmospheric lifetimes; and in situ bioassay experiments are highly valuable, particularly in unexplored key areas of the ocean.
4. How do differences in the physicochemical nature of different aerosol types alter their interactions with a similarly diverse suite of oceanic physical, chemical, and biological processes?
5. What are the responses of NPP and the biological pump to changes in aerosol fluxes from different sources in the context of a changing ocean physical state?

DISCLOSURE STATEMENT

The authors are not aware of any affiliations, memberships, funding, or financial holdings that might be perceived as affecting the objectivity of this review.

AUTHOR CONTRIBUTIONS

D.S.H. designed the article, provided MIMI modeling results, and created all figures and tables except **Figure 4** (created by R.W.) and **Figure 6** (created by N.O.). M.M.G.P. and A.R.B. provided Mount Wellington observations. R.R.B. provided QFED fire emissions. C.G. compiled in situ bioassay observation data. A.I. provided IMPACT modeling results. W.M. provided fire observation data used in **Supplemental Figures 1–3**. S.M. provided TM4 modeling results. K.S. and R.W. estimated dust emissions from fires. A.T. provided PISCES modeling results. Sections

Supplemental Material >

were jointly written as follows: Introduction (D.S.H., M.M.G.P., C.G., N.M.M., K.S., and A.T.); Aerosol Nutrients, Observations over Oceans, and Impacts on Biota (D.S.H., C.G., and A.T.); The Complex Interplay of Dust and Fire Aerosol Sources (D.S.H., K.S., R.W., and M.M.G.P.); Volcanic Aerosol Impacts on Marine Nutrient Supply (N.O. and D.S.H.); Anthropocene Perturbations to Aerosol Nutrient Sources (D.S.H., S.D.R., and T.C.B.); The Organic Nutrient Fraction (S.M. and N.M.M.); Australia: A Major Nutrient Source to Southern Hemisphere Oceans (M.M.G.P., D.S.H., A.I., and A.T.). Once compiled, all authors reviewed and edited the manuscript drafts.

ACKNOWLEDGMENTS

We are very grateful to Alex Baker for the marine observations presented in **Figure 1** and to Louisa Emmons for supplying the FINN fire emission data. We also thank Michal Strzelec and Scott Meyerink for assisting with the Mount Wellington time series and Ross Herbert for discussions on Global Model of Aerosol Processes (GLOMAP) results. D.S.H. and N.M.M. acknowledge the support of NASA (grant IDS 80NSSC20K1674) and the Department of Energy (grants DE-SC0021302 and, with T.C.B. and S.D.R., DE-SC0016362). A.I. received funding from the Japan Society for the Promotion of Science's Grants-in-Aid for Scientific Research (KAKENHI) (grant 20H04329) and from the Integrated Research Program for Advancing Climate Models (TOUGOU) (grant JPMXD0717935715) of the Japanese Ministry of Education, Culture, Sports, Science, and Technology. K.S. and R.W. acknowledge funding from the Deutsche Forschungsgemeinschaft (grant SCHE 1678/5-1). A.T. received funding from the European Research Council under the European Union's Horizon 2020 research and innovation program (grant 724289) and from the National Environment Research Council (grants NE/S013547/1, NE/N009525/1, and NE/N001079/1). We would like to acknowledge high-performance computing support from Cheyenne (<https://doi.org/10.5065/D6RX99HX>), provided by the National Center for Atmospheric Research's Computational and Information Systems Laboratory, sponsored by the National Science Foundation. Aerosol sampling and analysis at Mount Wellington were supported by the Australian Research Council (grant FT130100037 to A.R.B.) and authorized by the Wellington Park Management Trust.

LITERATURE CITED

- Altieri KE, Fawcett SE, Hastings MG. 2021. Reactive nitrogen cycling in the atmosphere and ocean. *Annu. Rev. Earth Planet. Sci.* 49:513–40. <https://doi.org/10.1146/annurev-earth-083120-052147>
- Andreae MO. 2019. Emission of trace gases and aerosols from biomass burning – an updated assessment. *Atmos. Chem. Phys.* 19:8523–46. <https://doi.org/10.5194/acp-19-8523-2019>
- Atanassova I, Doerr SH. 2011. Changes in soil organic compound composition associated with heat-induced increases in soil water repellency. *Eur. J. Soil Sci.* 62:516–32. <https://doi.org/10.1111/j.1365-2389.2011.01350.x>
- Aumont O, Ethé C, Tagliabue A, Bopp L, Gehlen M. 2015. PISCES-v2: an ocean biogeochemical model for carbon and ecosystem studies. *Geosci. Model Dev.* 8:2465–513. <https://doi.org/10.5194/gmd-8-2465-2015>
- Baker AR, Adams C, Bell TG, Jickells TD, Ganzeveld L. 2013. Estimation of atmospheric nutrient inputs to the Atlantic Ocean from 50°N to 50°S based on large-scale field sampling: iron and other dust-associated elements. *Glob. Biogeochem. Cycles* 27:755–67. <https://doi.org/10.1002/gbc.20062>
- Baker AR, Croot PL. 2010. Atmospheric and marine controls on aerosol iron solubility in seawater. *Mar. Chem.* 120:4–13. <https://doi.org/10.1016/j.marchem.2008.09.003>
- Baker AR, Jickells TD. 2017. Atmospheric deposition of soluble trace elements along the Atlantic Meridional Transect (AMT). *Prog. Oceanogr.* 158:41–51. <https://doi.org/10.1016/j.pocean.2016.10.002>

- Baker AR, Jickells TD, Biswas KF, Weston K, French M. 2006. Nutrients in atmospheric aerosol particles along the Atlantic Meridional Transect. *Deep-Sea Res. II* 53:1706–19. <https://doi.org/10.1016/j.dsr2.2006.05.012>
- Baker AR, Virkkula A, Correia AL, Bollhoefer A, Kumar A, et al. 2014. Aerosol and rain composition and deposition. *SOLAS Project Integration*. https://www.bodc.ac.uk/solas_integration/implementation_products/group1/aerosol_rain
- Baker AR, Weston K, Kelly SD, Voss M, Streu P, Cape JN. 2007. Dry and wet deposition of nutrients from the tropical Atlantic atmosphere: links to primary productivity and nitrogen fixation. *Deep-Sea Res. I* 54:1704–20. <https://doi.org/10.1016/j.dsr.2007.07.001>
- Barkley AE, Prospero JM, Mahowald NM, Hamilton DS, Pependorf KJ, et al. 2019. African biomass burning is a substantial source of phosphorus deposition to the Amazon, Tropical Atlantic Ocean, and Southern Ocean. *PNAS* 116:16216–21. <https://doi.org/10.1073/pnas.1906091116>
- Bhattarai H, Saikawa E, Wan X, Zhu H, Ram K, et al. 2019. Levoglucosan as a tracer of biomass burning: recent progress and perspectives. *Atmos. Res.* 220:20–33. <https://doi.org/10.1016/j.atmosres.2019.01.004>
- Boer MM, Resco de Dios V, Bradstock RA. 2020. Unprecedented burn area of Australian mega forest fires. *Nat. Clim. Change* 10:171–72. <https://doi.org/10.1038/s41558-020-0716-1>
- Bowie AR, Lannuzel D, Remenyi TA, Wagener T, Lam PJ, et al. 2009. Biogeochemical iron budgets of the Southern Ocean south of Australia: decoupling of iron and nutrient cycles in the subantarctic zone by the summertime supply. *Glob. Biogeochem. Cycles* 23:GB4034. <https://doi.org/10.1029/2009GB003500>
- Boyd PW, Ellwood MJ. 2010. The biogeochemical cycle of iron in the ocean. *Nat. Geosci.* 3:675–82. <https://doi.org/10.1038/ngeo964>
- Boyd PW, Strzepek R, Chiswell S, Chang H, DeBruyn JM, et al. 2012. Microbial control of diatom bloom dynamics in the open ocean. *Geophys. Res. Lett.* 39:2–7. <https://doi.org/10.1029/2012GL053448>
- Boyd PW, Strzepek RF, Ellwood MJ, Hutchins DA, Nodder SD, et al. 2015. Why are biotic iron pools uniform across high- and low-iron pelagic ecosystems? *Glob. Biogeochem. Cycles* 29:1028–43. <https://doi.org/10.1002/2014GB005014>
- Brahney J, Mahowald NM, Ward DS, Ballantyne AP, Neff JC. 2015. Is atmospheric phosphorus pollution altering global alpine lake stoichiometry? *Glob. Biogeochem. Cycles* 29:1369–83. <https://doi.org/10.1002/2015GB005137>
- Bressac M, Guieu C. 2013. Post-depositional processes: What really happens to new atmospheric iron in the ocean's surface? *Glob. Biogeochem. Cycles* 27:859–70. <https://doi.org/10.1002/gbc.20076>
- Cao F, Zhang SC, Kawamura K, Liu X, Yang C, et al. 2017. Chemical characteristics of dicarboxylic acids and related organic compounds in PM_{2.5} during biomass-burning and non-biomass-burning seasons at a rural site of northeast China. *Environ. Pollut.* 231:654–62. <https://doi.org/10.1016/j.envpol.2017.08.045>
- Capone D, Zehr J, Paerl H, Bergman B, Carpenter E. 1997. *Trichodesmium*, a globally significant marine cyanobacterium. *Science* 276:1221–29. <https://doi.org/10.1126/science.276.5316.1221>
- Cassar N, Bender ML, Barnett BA, Fan S, Moxim WJ, et al. 2007. The Southern Ocean biological response to aeolian iron deposition. *Science* 317:1067–70. <https://doi.org/10.1126/science.1144602>
- Chitrakar R, Tezuka S, Sonoda A, Sakane K, Ooi K, Hirotsu T. 2006. Phosphate adsorption on synthetic goethite and akaganeite. *J. Colloid Interface Sci.* 298:602–8. <https://doi.org/10.1016/j.jcis.2005.12.054>
- Cong Z, Kawamura K, Kang S, Fu P. 2015. Penetration of biomass-burning emissions from South Asia through the Himalayas: new insights from atmospheric organic acids. *Sci. Rep.* 5:9580. <https://doi.org/10.1038/srep09580>
- Conway TM, Hamilton DS, Shelley RU, Aguilar-Islas AM, Landing WM, et al. 2019. Tracing and constraining anthropogenic aerosol iron fluxes to the North Atlantic Ocean using iron isotopes. *Nat. Commun.* 10:2628. <https://doi.org/10.1038/s41467-019-10457-w>
- de Baar HJW, Boyd PW, Coale KH, Landry MR, Tsuda A, et al. 2005. Synthesis of iron fertilization experiments: from the iron age in the age of enlightenment. *J. Geophys. Res. C* 110:C09S16. <https://doi.org/10.1029/2004JC002601>
- Després VR, Huffman JA, Burrows SM, Hoose C, Safatov AS, et al. 2012. Primary biological aerosol particles in the atmosphere: a review. *Tellus B* 64:15598. <https://doi.org/10.3402/tellusb.v64i0.15598>

- Di Virgilio G, Evans JP, Blake SAP, Armstrong M, Dowdy AJ, et al. 2019. Climate change increases the potential for extreme wildfires. *Geophys. Res. Lett.* 46:8517–26. <https://doi.org/10.1029/2019GL083699>
- Doney SC, Lima I, Feely RA, Glover DM, Lindsay K, et al. 2009. Mechanisms governing interannual variability in upper-ocean inorganic carbon system and air-sea CO₂ fluxes: physical climate and atmospheric dust. *Deep-Sea Res. II* 56:640–55. <https://doi.org/10.1016/j.dsr2.2008.12.006>
- Dowdy AJ, Ye H, Pepler A, Thatcher M, Osbrough SL, et al. 2019. Future changes in extreme weather and pyroconvection risk factors for Australian wildfires. *Sci. Rep.* 9:10073. <https://doi.org/10.1038/s41598-019-46362-x>
- Duce RA, Liss PS, Merrill JT, Atlas EL, Buat-Menard P, et al. 1991. The atmospheric input of trace species to the world ocean. *Glob. Biogeochem. Cycles* 5:193–259. <https://doi.org/10.1029/91GB01778>
- Duggen S, Croot P, Schacht U, Hoffmann L. 2007. Subduction zone volcanic ash can fertilize the surface ocean and stimulate phytoplankton growth: evidence from biogeochemical experiments and satellite data. *Geophys. Res. Lett.* 34:L01612. <https://doi.org/10.1029/2006GL027522>
- Duggen S, Olgun N, Croot P, Hoffmann L, Dietze H, et al. 2010. The role of airborne volcanic ash for the surface ocean biogeochemical iron-cycle: a review. *Biogeosciences* 7:827–44. <https://doi.org/10.5194/bg-7-827-2010>
- Dukes D, Gonzales HB, Ravi S, Grandstaff DE, Van Pelt RS, et al. 2018. Quantifying postfire aeolian sediment transport using rare earth element tracers. *J. Geophys. Res. Biogeosci.* 123:288–99. <https://doi.org/10.1002/2017JG004284>
- FAO (Food Agric. Organ. UN). 2017. *World fertilizer trends and outlook to 2020: summary report*. Rep., FAO, Rome. <http://www.fao.org/3/a-i6895e.pdf>
- Fishwick MP, Sedwick PN, Lohan MC, Worsfold PJ, Buck KN, et al. 2014. The impact of changing surface ocean conditions on the dissolution of aerosol iron. *Glob. Biogeochem. Cycles* 28:1235–50. <https://doi.org/10.1002/2014GB004921>
- For. Fire Manag. Vic. 2021. Past bushfires: a chronology of major bushfires in Victoria from 2013 back to 1851. *Forest Fire Management Victoria*. <https://www.ffm.vic.gov.au/history-and-incidents/past-bushfires>
- Fu W, Randerson JT, Moore JK. 2016. Climate change impacts on net primary production (NPP) and export production (EP) regulated by increasing stratification and phytoplankton community structure in the CMIP5 models. *Biogeosciences* 13:5151–70. <https://doi.org/10.5194/bg-13-5151-2016>
- Fung I, Meyn SK, Tegen I, Doney S, John J, Bishop J. 2000. Iron supply and demand in the upper ocean. *Glob. Biogeochem. Cycles* 14:281–95. <https://doi.org/10.1029/1999GB900059>
- Gabric AJ, Cropp RA, McTainsh GH, Johnston BM, Butler H, et al. 2010. Australian dust storms in 2002–2003 and their impact on Southern Ocean biogeochemistry. *Glob. Biogeochem. Cycles* 24:GB2005. <https://doi.org/10.1029/2009GB003541>
- Gaudichet A, Echalar F, Chatenet B, Quisefit JP, Malingre G, et al. 1995. Trace elements in tropical African savanna biomass burning aerosols. *J. Atmos. Chem.* 22:19–39. <https://doi.org/10.1007/BF00708179>
- Gazeau F, Ridame C, Van Wambeke F, Alliouane S, Stolpe C, et al. 2020. Impact of dust enrichment on Mediterranean plankton communities under present and future conditions of pH and temperature: an experimental overview. *Biogeosci. Discuss.* In review. <https://doi.org/10.5194/bg-2020-202>
- Geng H, Park Y, Hwang H, Kang S, Ro CU. 2009. Elevated nitrogen-containing particles observed in Asian dust aerosol samples collected at the marine boundary layer of the Bohai Sea and the Yellow Sea. *Atmos. Chem. Phys.* 9:6933–47. <https://doi.org/10.5194/acp-9-6933-2009>
- Ginoux P, Prospero JM, Gill TE, Hsu NC, Zhao M. 2012. Global-scale attribution of anthropogenic and natural dust sources and their emission rates based on MODIS Deep Blue aerosol products. *Rev. Geophys.* 50:RG3005. <https://doi.org/10.1029/2012RG000388>
- Giovagnetti V, Brunet C, Conversano F, Tramontano F, Obernosterer I, et al. 2013. Assessing the role of dust deposition on phytoplankton ecophysiology and succession in a low-nutrient low-chlorophyll ecosystem: a mesocosm experiment in the mediterranean sea. *Biogeosciences* 10:2973–91. <https://doi.org/10.5194/bg-10-2973-2013>
- Graham B, Guyon P, Maenhaut W, Taylor PE, Ebert M, et al. 2003. Composition and diurnal variability of the natural Amazonian aerosol. *J. Geophys. Res. Atmos.* 108:4765. <https://doi.org/10.1029/2003JD004049>

- Guieu C, Al Azhar M, Aumont O, Mahowald NM, Levy M, et al. 2019. Major impact of dust deposition on the productivity of the Arabian Sea. *Geophys. Res. Lett.* 46:6736–44. <https://doi.org/10.1029/2019GL082770>
- Guieu C, Aumont O, Paytan A, Bopp L, Law CS, et al. 2014a. The significance of the episodic nature of atmospheric deposition to Low Nutrient Low Chlorophyll regions. *Glob. Biogeochem. Cycles* 28:1179–98. <https://doi.org/10.1002/2014GB004852>
- Guieu C, Bonnet S, Wagener T, Løjve-Pilot MD. 2005. Biomass burning as a source of dissolved iron to the open ocean? *Geophys. Res. Lett.* 32:L19608. <https://doi.org/10.1029/2005GL022962>
- Guieu C, Dulac F, Desboeufs K, Wagener T, Pulido-Villena E, et al. 2010. Large clean mesocosms and simulated dust deposition: a new methodology to investigate responses of marine oligotrophic ecosystems to atmospheric inputs. *Biogeosciences* 7:2765–84. <https://doi.org/10.5194/bg-7-2765-2010>
- Guieu C, Ridame C, Pulido-Villena E, Bressac M, Desboeufs K, Dulac F. 2014b. Impact of dust deposition on carbon budget: a tentative assessment from a mesocosm approach. *Biogeosciences* 11:5621–35. <https://doi.org/10.5194/bg-11-5621-2014>
- Hamilton DS, Hantson S, Scott CE, Kaplan JO, Pringle KJ, et al. 2018. Reassessment of pre-industrial fire emissions strongly affects anthropogenic aerosol forcing. *Nat. Commun.* 9:3182. <https://doi.org/10.1038/s41467-018-05592-9>
- Hamilton DS, Lee LA, Pringle KJ, Reddington CL, Spracklen DV, Carslaw KS. 2014. Occurrence of pristine aerosol environments on a polluted planet. *PNAS* 111:18466–71. <https://doi.org/10.1073/pnas.1415440111>
- Hamilton DS, Moore JK, Arneth A, Bond TC, Carslaw KS, et al. 2020a. Impact of changes to the atmospheric soluble iron deposition flux on ocean biogeochemical cycles in the Anthropocene. *Glob. Biogeochem. Cycles* 34:e2019GB006448. <https://doi.org/10.1029/2019GB006448>
- Hamilton DS, Scanza RA, Feng Y, Guinness J, Kok JF, et al. 2019. Improved methodologies for Earth system modelling of atmospheric soluble iron and observation comparisons using the Mechanism of Intermediate complexity for Modelling Iron (MIMI v1.0). *Geosci. Model Dev.* 12:3835–62. <https://doi.org/10.5194/gmd-12-3835-2019>
- Hamilton DS, Scanza RA, Rathod SD, Bond TC, Kok JF, et al. 2020b. Recent (1980 to 2015) trends and variability in daily-to-interannual soluble iron deposition from dust, fire, and anthropogenic sources. *Geophys. Res. Lett.* 47:e2020GL089688. <https://doi.org/10.1029/2020GL089688>
- Herbert RJ, Krom MD, Carslaw KS, Stockdale A, Mortimer RJG, et al. 2018. The effect of atmospheric acid processing on the global deposition of bioavailable phosphorus from dust. *Glob. Biogeochem. Cycles* 32:1367–85. <https://doi.org/10.1029/2018GB005880>
- Hoffmann LJ, Breitbarth E, Ardelan MV, Duggen S, Olgun N, et al. 2012. Influence of trace metal release from volcanic ash on growth of *Thalassiosira pseudonana* and *Emiliania huxleyi*. *Mar. Chem.* 132–33:28–33. <https://doi.org/10.1016/j.marchem.2012.02.003>
- Ito A. 2015. Atmospheric processing of combustion aerosols as a source of bioavailable iron. *Environ. Sci. Technol. Lett.* 2:70–75. <https://doi.org/10.1021/acs.estlett.5b00007>
- Ito A, Adebisi AA, Huang Y, Kok JF. 2021. Less atmospheric radiative heating due to aspherical dust with coarser size. *Atmos. Chem. Phys. Discuss.* In review. <https://doi.org/10.5194/acp-2021-134>
- Ito A, Lin G, Penner JE. 2018. Radiative forcing by light-absorbing aerosols of pyrogenic iron oxides. *Sci. Rep.* 8:7347. <https://doi.org/10.1038/s41598-018-25756-3>
- Ito A, Myriokefalitakis S, Kanakidou M, Mahowald NM, Scanza RA, et al. 2019. Pyrogenic iron: the missing link to high iron solubility in aerosols. *Sci. Adv.* 5:eaau7671. <https://doi.org/10.1126/sciadv.aau7671>
- Ito A, Perron MMG, Proemse BC, Strzelec M, Gault-Ringold M, et al. 2020a. Evaluation of aerosol iron solubility over Australian coastal regions based on inverse modeling: implications of bushfires on bioaccessible iron concentrations in the Southern Hemisphere. *Prog. Earth Planet. Sci.* 7:42. <https://doi.org/10.1186/s40645-020-00357-9>
- Ito A, Shi Z. 2016. Delivery of anthropogenic bioavailable iron from mineral dust and combustion aerosols to the ocean. *Atmos. Chem. Phys.* 16:85–99. <https://doi.org/10.5194/acp-16-85-2016>
- Ito A, Ye Y, Yamamoto A, Watanabe M, Aita MN. 2020b. Responses of ocean biogeochemistry to atmospheric supply of lithogenic and pyrogenic iron-containing aerosols. *Geol. Mag.* 157:741–56. <https://doi.org/10.1017/S0016756819001080>

- Jaenicke R, Matthias-Maser S, Gruber S. 2007. Omnipresence of biological material in the atmosphere. *Environ. Chem.* 4:217–20. <https://doi.org/10.1071/EN07021>
- Jeanneau AC, Ostendorf B, Herrmann T. 2019. Relative spatial differences in sediment transport in fire-affected agricultural landscapes: a field study. *Aeolian Res.* 39:13–22. <https://doi.org/10.1016/j.aeolia.2019.04.002>
- Jickells TD, An ZS, Andersen KK, Baker AR, Bergametti G, et al. 2005. Global iron connections between desert dust, ocean biogeochemistry, and climate. *Science* 308:67–71. <https://doi.org/10.1126/science.1105959>
- Jickells TD, Buitenhuis E, Altieri K, Baker AR, Capone D, et al. 2017. A reevaluation of the magnitude and impacts of anthropogenic atmospheric nitrogen inputs on the ocean. *Glob. Biogeochem. Cycles* 31:289–305. <https://doi.org/10.1002/2016GB005586>
- Johnson MS, Meshkidze N. 2013. Atmospheric dissolved iron deposition to the global oceans: effects of oxalate-promoted Fe dissolution, photochemical redox cycling, and dust mineralogy. *Geosci. Model. Dev.* 6:1137–55. <https://doi.org/10.5194/gmd-6-1137-2013>
- Journet E, Balkanski Y, Harrison SP. 2014. A new data set of soil mineralogy for dust-cycle modeling. *Atmos. Chem. Phys.* 14:3801–16. <https://doi.org/10.5194/acp-14-3801-2014>
- Journet E, Desbouefs K, Caquineau S, Colin J-L. 2008. Mineralogy as a critical factor of dust iron solubility. *Geophys. Res. Lett.* 35:L07805. <https://doi.org/10.1029/2007GL031589>
- Kanakidou M, Duce RA, Prospero JM, Baker AR, Benitez-Nelson C, et al. 2012. Atmospheric fluxes of organic N and P to the global ocean. *Glob. Biogeochem. Cycles* 26:GB3026. <https://doi.org/10.1029/2011GB004277>
- Kanakidou M, Myriokefalitakis S, Daskalakis N, Fanourgakis G, Nenes A, et al. 2016. Past, present, and future atmospheric nitrogen deposition. *J. Atmos. Sci.* 73:2039–47. <https://doi.org/10.1175/JAS-D-15-0278.1>
- Kanakidou M, Myriokefalitakis S, Tsigaridis K. 2018. Aerosols in atmospheric chemistry and biogeochemical cycles of nutrients. *Environ. Res. Lett.* 13:063004. <https://doi.org/10.1088/1748-9326/aabcbdb>
- Kavouras IG, Nikolich G, Etyemezian V, Dubois DW, King J, Shafer D. 2012. In situ observations of soil minerals and organic matter in the early phases of prescribed fires. *J. Geophys. Res. Atmos.* 117:D12313. <https://doi.org/10.1029/2011JD017420>
- Khaykin S, Legras B, Bucci S, Sellitto P, Isaksen I, et al. 2020. The 2019/20 Australian wildfires generated a persistent smoke-charged vortex rising up to 35 km altitude. *Commun. Earth Environ.* 1:22. <https://doi.org/10.1038/s43247-020-00022-5>
- Kok JF, Adebisi AA, Albani S, Balkanski Y, Checa-Garcia R, et al. 2021. Contribution of the world's main dust source regions to the global cycle of desert dust. *Atmos. Chem. Phys.* 21:8169–93. <https://doi.org/10.5194/acp-21-8169-2021>
- Krishnamurthy A, Moore JK, Mahowald NM, Luo C, Doney SC, et al. 2009. Impacts of increasing anthropogenic soluble iron and nitrogen deposition on ocean biogeochemistry. *Glob. Biogeochem. Cycles* 23:GB3016. <https://doi.org/10.1029/2008GB003440>
- Kundu S, Kawamura K, Andreae TW, Hoffer A, Andreae MO. 2010. Diurnal variation in the water-soluble inorganic ions, organic carbon and isotopic compositions of total carbon and nitrogen in biomass burning aerosols from the LBA-SMOCC campaign in Rondônia, Brazil. *J. Aerosol Sci.* 41:118–33. <https://doi.org/10.1016/j.jaerosci.2009.08.006>
- La Roche J, Breitbarth E. 2005. Importance of the diazotrophs as a source of new nitrogen in the ocean. *J. Sea Res.* 53:67–91. <https://doi.org/10.1016/j.seares.2004.05.005>
- Lamb KD, Matsui H, Katich JM, Perring AE, Spackman JR, et al. 2021. Global-scale constraints on light-absorbing anthropogenic iron oxide aerosols. *npj Clim. Atmos. Sci.* 4:15. <https://doi.org/10.1038/s41612-021-00171-0>
- Langmann B. 2013. Volcanic ash versus mineral dust: atmospheric processing and environmental and climate impacts. *ISRN Atmos. Sci.* 2013:245076. <https://doi.org/10.1155/2013/245076>
- Lasaga AC, Soler JM, Ganor J, Burch TE, Nagy KL. 1994. Chemical weathering rate laws and global geochemical cycles. *Geochim. Cosmochim. Acta* 58:2361–86. [https://doi.org/10.1016/0016-7037\(94\)90016-7](https://doi.org/10.1016/0016-7037(94)90016-7)

- Letelier RM, Björkman KM, Church MJ, Hamilton DS, Mahowald NM, et al. 2019. Climate-driven oscillation of phosphorus and iron limitation in the North Pacific Subtropical Gyre. *PNAS* 116:12720–28. <https://doi.org/10.1073/pnas.1900789116>
- Li W, Xu L, Liu X, Zhang J, Lin Y, et al. 2017. Air pollution–aerosol interactions produce more bioavailable iron for ocean ecosystems. *Sci. Adv.* 3:e1601749. <https://doi.org/10.1126/sciadv.1601749>
- Longo AF, Feng Y, Lai B, Landing WM, Shelley RU, et al. 2016. Influence of atmospheric processes on the solubility and composition of iron in Saharan dust. *Environ. Sci. Technol.* 50:6912–20. <https://doi.org/10.1021/acs.est.6b02605>
- Louis J, Bressac M, Pedrotti ML, Guieu C. 2015. Dissolved inorganic nitrogen and phosphorus dynamics in seawater following an artificial Saharan dust deposition event. *Front. Mar. Sci.* 2:27. <https://doi.org/10.3389/fmars.2015.00027>
- Louis J, Gazeau F, Guieu C. 2018. Atmospheric nutrients in seawater under current and high $p\text{CO}_2$ conditions after Saharan dust deposition: results from three minicosm experiments. *Prog. Oceanogr.* 163:40–49. <https://doi.org/10.1016/j.pocean.2017.10.011>
- Lucas J, Harris RMB. 2021. Changing climate suitability for dominant Eucalyptus species may affect future fuel loads and flammability in Tasmania. *Fire* 4:1. <https://doi.org/10.3390/fire4010001>
- Luo C, Mahowald NM, Bond T, Chuang PY, Artaxo P, et al. 2008. Combustion iron distribution and deposition. *Glob. Biogeochem. Cycles* 22:GB1012. <https://doi.org/10.1029/2007GB002964>
- Mackie DS, Boyd PW, McTainsh GH, Tindale NW, Westberry TK, Hunter KA. 2008. Biogeochemistry of iron in Australian dust: from eolian uplift to marine uptake. *Geochem. Geophys. Geosyst.* 9:Q03Q08. <https://doi.org/10.1029/2007GC001813>
- Maenhaut W, Salma I, Cafineyer J, Annegarn HJ, Andreae MO. 1996. Regional atmospheric aerosol composition and sources in the eastern Transvaal, South Africa, and impact of biomass burning. *J. Geophys. Res. Atmos.* 101:23631–50. <https://doi.org/10.1029/95jd02930>
- Mahowald NM, Artaxo P, Baker AR, Jickells TD, Okin GS, et al. 2005. Impacts of biomass burning emissions and land use change on Amazonian atmospheric phosphorus cycling and deposition. *Glob. Biogeochem. Cycles* 19:GB4030. <https://doi.org/10.1029/2005GB002541>
- Mahowald NM, Engelstaedter S, Luo C, Sealy A, Artaxo P, et al. 2009. Atmospheric iron deposition: global distribution, variability, and human perturbations. *Annu. Rev. Mar. Sci.* 1:245–78. <https://doi.org/10.1146/annurev.marine.010908.163727>
- Mahowald NM, Hamilton DS, Mackey KRM, Moore JK, Baker AR, et al. 2018. Aerosol trace metal leaching and impacts on marine microorganisms. *Nat. Commun.* 9:2614. <https://doi.org/10.1038/s41467-018-04970-7>
- Mahowald NM, Jickells TD, Baker AR, Artaxo P, Benitez-Nelson CR, et al. 2008. Global distribution of atmospheric phosphorus sources, concentrations and deposition rates, and anthropogenic impacts. *Glob. Biogeochem. Cycles* 22:GB4026. <https://doi.org/10.1029/2008GB003240>
- Mahowald NM, Kloster S, Engelstaedter S, Moore JK, Mukhopadhyay S, et al. 2010. Observed 20th century desert dust variability: impact on climate and biogeochemistry. *Atmos. Chem. Phys.* 10:10875–93. <https://doi.org/10.5194/acp-10-10875-2010>
- Marañón E, Fernández A, Mouriño-Carballido B, Martínez-García S, Teira E, et al. 2010. Degree of oligotrophy controls the response of microbial plankton to Saharan dust. *Limnol. Oceanogr.* 55:2339–52. <https://doi.org/10.4319/lo.2010.55.6.2339>
- Martin H, Gordon RM, Fitzwater SE. 1991. The case for iron. *Limnol. Ocean.* 36:1793–802. <https://doi.org/10.4319/lo.1991.36.8.1793>
- Martin J. 1990. Glacial-interglacial CO_2 change: the iron hypothesis. *Paleoceanography* 5:1–13. <https://doi.org/10.1029/PA005i001p00001>
- Matsui H, Mahowald NM, Moteki N, Hamilton DS, Ohata S, et al. 2018. Anthropogenic combustion iron as a complex climate forcer. *Nat. Commun.* 9:1593. <https://doi.org/10.1038/s41467-018-03997-0>
- McLennan SM. 2001. Relationships between the trace element composition of sedimentary rocks and upper continental crust. *Geochem. Geophys. Geosyst.* 2:1021. <https://doi.org/10.1029/2000GC000109>
- McNabb DH, Swanson FJ. 1990. Effects of fire on soil erosion. In *Natural and Prescribed Fire in Pacific Northwest Forests*, ed. JD Walstad, DV Sandberg, SR Radosevich, pp. 159–176. Corvallis: Or. State Univ. Press

- Meskhidze N, Chameides WL, Nenes A. 2005. Dust and pollution: a recipe for enhanced ocean fertilization? *J. Geophys. Res. Atmos.* 110:D03301. <https://doi.org/10.1029/2004JD005082>
- Moore CM, Mills MM, Arrigo KR, Berman-Frank I, Bopp L, et al. 2013. Processes and patterns of oceanic nutrient limitation. *Nat. Geosci.* 6:701–10. <https://doi.org/10.1038/ngeo1765>
- Myriokefalitakis S, Daskalakis N, Mihalopoulos N, Baker AR, Nenes A, Kanakidou M. 2015. Changes in dissolved iron deposition to the oceans driven by human activity: a 3-D global modelling study. *Biogeosciences* 12:3973–92. <https://doi.org/10.5194/bg-12-3973-2015>
- Myriokefalitakis S, Gröger M, Hieronymus J, Döscher R. 2020. An explicit estimate of the atmospheric nutrient impact on global oceanic productivity. *Ocean Sci.* 16:1183–205. <https://doi.org/10.5194/os-16-1183-2020>
- Myriokefalitakis S, Ito A, Kanakidou M, Nenes A, Krol MC, et al. 2018. Reviews and syntheses: the GESAMP atmospheric iron deposition model intercomparison study. *Biogeosciences* 15:6659–84. <https://doi.org/10.5194/bg-15-6659-2018>
- Myriokefalitakis S, Nenes A, Baker AR, Mihalopoulos N, Kanakidou M. 2016. Bioavailable atmospheric phosphorous supply to the global ocean: a 3-D global modeling study. *Biogeosciences* 13:6519–43. <https://doi.org/10.5194/bg-13-6519-2016>
- Myriokefalitakis S, Tsigaridis K, Mihalopoulos N, Sciare J, Nenes A, et al. 2011. In-cloud oxalate formation in the global troposphere: a 3-D modeling study. *Atmos. Chem. Phys.* 11:5761–82. <https://doi.org/10.5194/acp-11-5761-2011>
- Nenes A, Krom MD, Mihalopoulos N, Van Cappellen P, Shi Z, et al. 2011. Atmospheric acidification of mineral aerosols: a source of bioavailable phosphorus for the oceans. *Atmos. Chem. Phys.* 11:6265–72. <https://doi.org/10.5194/acp-11-6265-2011>
- Nisantzi A, Mamouri RE, Ansmann A, Hadjimitsis D. 2014. Injection of mineral dust into the free troposphere during fire events observed with polarization lidar at Limassol, Cyprus. *Atmos. Chem. Phys.* 14:12155–65. <https://doi.org/10.5194/acp-14-12155-2014>
- Oakes M, Ingall ED, Lai B, Shafer MM, Hays MD, et al. 2012. Iron solubility related to particle sulfur content in source emission and ambient fine particles. *Environ. Sci. Technol.* 46:6637–44. <https://doi.org/10.1021/es300701c>
- Olgun N, Duggen S, Andronico D, Kutterolf S, Croot PL, et al. 2013. Possible impacts of volcanic ash emissions of Mount Etna on the primary productivity in the oligotrophic Mediterranean Sea: results from nutrient-release experiments in seawater. *Mar. Chem.* 152:32–42. <https://doi.org/10.1016/j.marchem.2013.04.004>
- Olgun N, Duggen S, Croot PL, Delmelle P, Dietze H, et al. 2011. Surface ocean iron fertilization: the role of airborne volcanic ash from subduction zone and hot spot volcanoes and related iron fluxes into the Pacific Ocean. *Glob. Biogeochem. Cycles* 25:GB4001. <https://doi.org/10.1029/2009GB003761>
- Parekh P, Follows MJ, Boyle E. 2004. Modeling the global ocean iron cycle. *Glob. Biogeochem. Cycles* 18:GB1002. <https://doi.org/10.1029/2003gb002061>
- Paris R, Desboeufs KV, Formenti P, Nava S, Chou C. 2010. Chemical characterisation of iron in dust and biomass burning aerosols during AMMA-SOP0/DABEX: implication for iron solubility. *Atmos. Chem. Phys.* 10:4273–82. <https://doi.org/10.5194/acp-10-4273-2010>
- Paytan A, Mackey KRM, Chen Y, Lima ID, Doney SC, et al. 2009. Toxicity of atmospheric aerosols on marine phytoplankton. *PNAS* 106:4601–5. <https://doi.org/10.1073/pnas.0811486106>
- Pérez-Cabello F, de la Riva Fernández J, Montorio Llovería R, García-Martín A. 2006. Mapping erosion-sensitive areas after wildfires using fieldwork, remote sensing, and geographic information systems techniques on a regional scale. *J. Geophys. Res. Biogeosci.* 111:G04S10. <https://doi.org/10.1029/2005JG000148>
- Perron MMG, Proemse BC, Strzelec M, Gault-Ringold M, Boyd PW, et al. 2020. Origin, transport and deposition of aerosol iron to Australian coastal waters. *Atmos. Environ.* 228:117432. <https://doi.org/10.1016/j.atmosenv.2020.117432>
- Ramos ME, Garcia-Palma S, Rozalen M, Johnston CT, Huertas FJ. 2014. Kinetics of montmorillonite dissolution: an experimental study of the effect of oxalate. *Chem. Geol.* 363:283–92. <https://doi.org/10.1016/j.chemgeo.2013.11.014>

- Rathod SD, Hamilton DS, Mahowald NM, Klimont Z, Corbett JJ, Bond TC. 2020. A mineralogy-based anthropogenic combustion-iron emission inventory. *J. Geophys. Res. Atmos.* 125:e2019JD032114. <https://doi.org/10.1029/2019jd032114>
- Reid JS, Koppmann R, Eck TF, Eleuterio DP. 2005. A review of biomass burning emissions part II: intensive physical properties of biomass burning particles. *Atmos. Chem. Phys.* 5:799–825. <https://doi.org/10.5194/acp-5-799-2005>
- Sarmiento JL, Gruber N, Brzezinski MA, Dunne JP. 2004. High-latitude controls of thermocline nutrients and low latitude biological productivity. *Nature* 427:56–60. <https://doi.org/10.1038/nature02127>
- Schlosser JS, Braun RA, Bradley T, Dadashazar H, MacDonald AB, et al. 2017. Analysis of aerosol composition data for western United States wildfires between 2005 and 2015: dust emissions, chloride depletion, and most enhanced aerosol constituents. *J. Geophys. Res. Atmos.* 122:8951–66. <https://doi.org/10.1002/2017JD026547>
- Schmidl C, Marr IL, Caseiro A, Kotianová P, Berner A, et al. 2008. Chemical characterisation of fine particle emissions from wood stove combustion of common woods growing in mid-European Alpine regions. *Atmos. Environ.* 42:126–41. <https://doi.org/10.1016/j.atmosenv.2007.09.028>
- Shi Z, Bonneville S, Krom MD, Carslaw KS, Jickells TD, et al. 2011. Iron dissolution kinetics of mineral dust at low pH during simulated atmospheric processing. *Atmos. Chem. Phys.* 11:995–1007. <https://doi.org/10.5194/acp-11-995-2011>
- Shi Z, Krom MD, Bonneville S, Benning LG. 2015. Atmospheric processing outside clouds increases soluble iron in mineral dust. *Environ. Sci. Technol.* 49:1472–77. <https://doi.org/10.1021/es504623x>
- Solmon F, Chuang PY, Meskhidze N, Chen Y. 2009. Acidic processing of mineral dust iron by anthropogenic compounds over the north Pacific Ocean. *J. Geophys. Res.* 114:D02305. <https://doi.org/10.1029/2008JD010417>
- Stockdale A, Krom MD, Mortimer RJG, Benning LG, Carslaw KS, et al. 2016. Understanding the nature of atmospheric acid processing of mineral dusts in supplying bioavailable phosphorus to the oceans. *PNAS* 113:14639–44. <https://doi.org/10.1073/pnas.1608136113>
- Straub SM, Schmincke HU. 1998. Evaluating the tephra input into Pacific Ocean sediments: distribution in space and time. *Int. J. Earth Sci.* 87:461–76. <https://doi.org/10.1007/s005310050222>
- Strzelec M, Proemse BC, Gault-Ringold M, Boyd PW, Perron MMG, et al. 2020. Atmospheric trace metal deposition near the Great Barrier Reef, Australia. *Atmosphere* 11:390. <https://doi.org/10.3390/ATMOS11040390>
- Tagliabue A, Aumont O, Bopp L. 2014. The impact of different external sources of iron on the global carbon cycle. *Geophys. Res. Lett.* 41:920–26. <https://doi.org/10.1002/2013GL059059>
- Tagliabue A, Bopp L, Aumont O. 2008. Ocean biogeochemistry exhibits contrasting responses to a large scale reduction in dust deposition. *Biogeosciences* 5:11–24. <https://doi.org/10.5194/bg-5-11-2008>
- Tagliabue A, Bopp L, Roche D, Bouttes N, Dutay J-C, et al. 2009. Quantifying the roles of ocean circulation and biogeochemistry in governing ocean carbon-13 and atmospheric carbon dioxide at the last glacial maximum. *Clim. Past* 5:695–706. <https://doi.org/10.5194/cp-5-695-2009>
- Tagliabue A, Bowie AR, Boyd PW, Buck KN, Johnson KS, Saito MA. 2017. The integral role of iron in ocean biogeochemistry. *Nature* 543:51–59. <https://doi.org/10.1038/nature21058>
- Textor C, Schulz M, Guibert S, Kinne S, Balkanski Y, et al. 2006. Analysis and quantification of the diversities of aerosol life cycles within AeroCom. *Atmos. Chem. Phys.* 6:1777–813. <https://doi.org/10.5194/acpd-5-8331-2005>
- Tipping E, Benham S, Boyle JF, Crow P, Davies J, et al. 2014. Atmospheric deposition of phosphorus to land and freshwater. *Environ. Sci. Process. Impacts* 16:1608–17. <https://doi.org/10.1039/c3em00641g>
- Twining BS, Antipova O, Chappell PD, Cohen NR, Jacquot JE, et al. 2020. Taxonomic and nutrient controls on phytoplankton iron quotas in the ocean. *Limnol. Oceanogr. Lett.* 6:96–106. <https://doi.org/10.1002/lo2.10179>
- Twining BS, Baines SB. 2013. The trace metal composition of marine phytoplankton. *Annu. Rev. Mar. Sci.* 5:191–215. <https://doi.org/10.1146/annurev-marine-121211-172322>
- Uetake J, Hill TCJ, Moore KA, DeMott PJ, Protat A, Kreidenweis SM. 2020. Airborne bacteria confirm the pristine nature of the Southern Ocean boundary layer. *PNAS* 117:13275–82. <https://doi.org/10.1073/pnas.2000134117>

- Wagenbrenner NS, Chung SH, Lamb BK. 2017. A large source of dust missing in particulate matter emission inventories? Wind erosion of post-fire landscapes. *Elem. Sci. Anthr.* 5:2. <https://doi.org/10.1525/elementa.185>
- Wagener T, Guieu C, Leblond N. 2010. Effects of dust deposition on iron cycle in the surface Mediterranean Sea: results from a mesocosm seeding experiment. *Biogeosciences* 7:3769–81. <https://doi.org/10.5194/bg-7-3769-2010>
- Wagener T, Pulido-Villena E, Guieu C. 2008. Dust iron dissolution in seawater: results from a one-year time-series in the Mediterranean Sea. *Geophys. Res. Lett.* 35:L16601. <https://doi.org/10.1029/2008GL034581>
- Wagner R, Jähn M, Schepanski K. 2018. Wildfires as a source of airborne mineral dust – revisiting a conceptual model using large-eddy simulation (LES). *Atmos. Chem. Phys.* 18:11863–84. <https://doi.org/10.5194/acp-18-11863-2018>
- Wang R, Balkanski Y, Bopp L, Aumont O, Boucher O, et al. 2015. Influence of anthropogenic aerosol deposition on the relationship between oceanic productivity and warming. *Geophys. Res. Lett.* 42:10745–54. <https://doi.org/10.1002/2015GL066753>
- Ward DS, Mahowald NM, Kloster S. 2014. Potential climate forcing of land use and land cover change. *Atmos. Chem. Phys.* 14:12701–24. <https://doi.org/10.5194/acp-14-12701-2014>
- Whicker JJ, Pinder JE, Breshears DD. 2006. Increased wind erosion from forest wildfire: implications for contaminant-related risks. *J. Environ. Qual.* 35:468–78. <https://doi.org/10.2134/jeq2005.0112>
- Winton VHL, Bowie AR, Edwards R, Keywood M, Townsend AT, et al. 2015. Fractional iron solubility of atmospheric iron inputs to the Southern Ocean. *Mar. Chem.* 177:20–32. <https://doi.org/10.1016/j.marchem.2015.06.006>
- Winton VHL, Edwards R, Bowie AR, Keywood M, Williams AG, et al. 2016. Dry season aerosol iron solubility in tropical northern Australia. *Atmos. Chem. Phys.* 16:12829–48. <https://doi.org/10.5194/acp-16-12829-2016>
- Wu C, Lin Z, Liu X. 2020. The global dust cycle and uncertainty in CMIP5 (Coupled Model Intercomparison Project) models. *Atmos. Chem. Phys.* 20:10401–25. <https://doi.org/10.5194/acp-20-10401-2020>
- Yamasoe MA, Artaxo P, Miguel AH, Allen AG. 2000. Chemical composition of aerosol particles from direct emissions of vegetation fires in the Amazon Basin: water-soluble species and trace elements. *Atmos. Environ.* 34:1641–53. [https://doi.org/10.1016/S1352-2310\(99\)00329-5](https://doi.org/10.1016/S1352-2310(99)00329-5)
- Ye Y, Völker C. 2017. On the role of dust-deposited lithogenic particles for iron cycling in the tropical and subtropical Atlantic. *Glob. Biogeochem. Cycles* 31:1543–58. <https://doi.org/10.1002/2017GB005663>
- Zhang C, Ito A, Shi Z, Aita MN, Yao X, et al. 2019. Fertilization of the Northwest Pacific Ocean by East Asia air pollutants. *Glob. Biogeochem. Cycles* 33:690–702. <https://doi.org/10.1029/2018GB006146>